Recent progress on fabrication and drug delivery applications of nanostructured hydroxyapatite

Sudip Mondal,[1] Sergy V. Dorozhkin[2] and Umapada Pal[1]*

Through this brief review, we provide a comprehensive historical background of the development of nanostructured hydroxyapatite (nHAp), and its application potentials for controlled drug delivery, drug conjugation, and other biomedical treatments. Aspects associated with efficient utilization of hydroxyapatite (HAp) nanostructures such as their synthesis, interaction with drug molecules, and other concerns, which need to be resolved before they could be used as a potential drug carrier in body system, are discussed. This review focuses on the evolution of perceptions, practices, and accomplishments in providing improved delivery systems for drugs until date. The pioneering developments that have presaged today's fascinating state of the art drug delivery systems based on HAp and HAp-based composite nanostructures are also discussed. Special emphasis has been given to describe the application and effectiveness of modified HAp as drug carrier agent for different diseases such as bone-related disorders, carriers for antibiotics, anti-inflammatory, carcinogenic drugs, medical imaging, and protein delivery agents. As only a very few published works made comprehensive evaluation of HAp nanostructures for drug delivery applications, we try to cover the three major areas: concepts, practices and achievements, and applications, which have been consolidated and patented for their practical usage. The review covers a broad spectrum of nHAp and HAp modified inorganic drug carriers, emphasizing some of their specific aspects those needed to be considered for future drug delivery applications. © 2017 Wiley Periodicals, Inc.

INTRODUCTION

After more than two decades of scientific innovation through research and development, nanotechnology has restructured the traditional philosophy of using ceramics in medical sciences. From the very early stage of healthcare industry, polymers played a key role in drug delivery. The prospering of nanotechnology rejuvenated the performance of ceramic materials, enhancing their

potentiality for loading and releasing of numerous drugs in affected tissues. During the last few years, advances in nanophase ceramics achieved their applications in healthcare, tissue engineering, and other biomedical fields. Different ceramics such as alumina (Al_2O_3), titania (TiO_2), zirconia (ZrO_2), calcium phosphates (CaP), and bioactive glasses have made substantial contributions for the improvement of present-day healthcare systems. Most of these ceramics, pristine or modified, have been used inside human body without major rejection. These bioceramics support to rejuvenate or augment several unhealthy or damaged tissues of the skeletal system. Applications of bioceramics have also been extended as bone substituted prosthetics and drug delivery agents in the biomedical arena due to their excellent

*Correspondence to: upal@ifuap.buap.mx

[1]Instituto de Física, Benemérita Universidad Autónoma de Puebla, Puebla, Mexico

[2]Kudrinskaja sq. 1–155, Moscow, Russia

Conflict of interest: The authors have declared no conflicts of interest for this article.

biocompatibility, bio-affinity, bioactivity, high stability, and adequate mechanical properties. The prospective of any ceramic material for healthcare application depends upon its ability to endure complex stresses at the site of application, drug transportation, controlled and prolonged release, and compatibility with biological surroundings. Recent advances in nanophase bioceramics, especially the calcium phosphates such as hydroxyapatite (HAp), are making drug delivery process more efficient, with the promise to solve many challenging medical problems.

History of Biomaterials

Utilization of biomaterials in healthcare applications is not a new invent for medical science. The early medical literature of the Hindu, Egyptian and Greek civilizations also indicate successful utilization of biomaterials as implants in the skeletal system.[1] Due to the lack of knowledge on good medical and scientific practice, the ancient selection of biomaterials was based on their accessibility and availabilities.[2] The application of ancient biomaterials such as corals, shells, ivory (elephant tusk), stone, wood, and some metals like gold and silver are found in museums, exhibited in archeological findings of animal or human mummies or cadavers. The Chinese were the first (659 AD) to use dental amalgam to repair decayed teeth; whereas, pre-Columbian civilizations used gold sheets to heal cranial cavities through trepanation (by surgical intervention a hole is drilled or scraped into the human skull).[3] Ambroise Pareʹ (1510–1590) described the measures to reconstruct teeth, noses, and other parts of the body in his work 'Dix livres de la chirurgie.' In 1970, Amadeo Bobbio discovered Mayan skulls, some of which were more than 4000 years old, in which missing teeth had been replaced by nacre substitutes.[4] The first modern use of plaster of Paris as bone substitute has been reported by Dressmann in 1892.[5] Nevertheless, the use of biomaterials did not become practical until these three milestone discoveries have been made:

- An aseptic surgical technique developed by J. Lister in the 1860s.
- Dependence of tissue regeneration on cell proliferation by Rudolf Virchow (1821–1902, in Cellular pathologie).
- *In vitro* cell cultivation by R.G. Harrison (1870–1959), demonstrating active growth of cells in culture medium.

In the modern era of biomaterials, Professor James M. Anderson introduced a classification on the progress of biomaterials' applications. According to him, during 1950–1975, the researchers studied bioMATERIALS, then, from 1975 to 2000, the progress has been made on BIOMATERIALS, and, since 2000, the time of BIOmaterials has been started.[6] The capital letters here emphasize the major direction of the research efforts in the multifaceted subject of biomaterials. In this frame, applications of CaP BIOmaterials appear to be rational due to their resemblance with the mineral phases of hard tissues. According to available literature, the first attempt to use them (it was tricalcium phosphate, TCP) as artificial material to repair surgically created defects in rabbits was performed in 1920.[7] In 1975, Nery et al. reported the first dental application of calcium orthophosphate in surgically created periodontal defects.[8] Among all the past, present and prospective bioceramics, CaPs have a significant contribution for the replacement of bones, knees, hips, teeth, and restoration of disorders associated with periodontal disease, maxillofacial reconstruction, and augmentation, stabilization of the spine and jawbones. Today, CaPs are the materials of choice for different pharmaceutical applications like tissue engineering, drug delivery, drug formulation, dentistry, and medicine. The available CaPs have been classified according to their chemical compositions, as described in Table 1.

Among different forms of CaP, particular attention has been paid to TCP ($Ca_3(PO_4)_2$) and HAp $Ca_{10}(PO_4)_6(OH)_2$), due to their excellent biological responses and resorbability in the physiological environments. The contemporary healthcare industry uses CaP ceramics in various applications, depending on their resorbability and bioactivity. Recent trend in bio-ceramic research is focused on overcoming the limitations of CaP, precisely HAp ceramics and improving their biological adaptability by exploring the unique advantages of nanotechnology. Among all the CaP phases, HAp is the most significant phase due to its chemical stability and extended biocompatibility. HAp has the lowest solubility and highest stability in aqueous media among other CaP phases. For example, the solubility value of HAp is at least 30 orders of magnitude lower than that of α-tricalcium phosphate (α-TCP).[13]

Ceramics as Drug Delivery Agents

The most substantial mandate for biomaterials has emerged as a significant need to provide clinical treatment to a great number of patients. The pursuit of probable solutions generated a strong demand for

TABLE 1 | Classification of Calcium Phosphate Salts

Chemical Name	Chemical Formula	Ca/P Molar Ratio	pH Stability in Aqueous (25°C)	Ref.
Monocalcium phosphate monohydrate (MCPM)	$Ca(H_2PO_4)_2 \cdot H_2O$	0.5	0.0–2.0	9
Monocalcium phosphate anhydrous (MCPA or MCP)	$Ca(H_2PO_4)_2$	0.5	Stable above 100 °C temperature	10
Dicalcium phosphate dihydrate (DCPD), mineral brushite	$CaHPO_4 \cdot 2H_2O$	1.0	2.0–6.0	11
Dicalcium phosphate anhydrous (DCPA or DCP), mineral monetite	$CaHPO_4$	1.0	Stable above 100 °C temperature	12
Octacalcium phosphate (OCP)	$Ca_8(HPO_4)_2(PO_4)_4 \cdot 5H_2O$	1.33	5.5–7.0	11
α-Tricalcium phosphate (α-TCP)	$\alpha\text{-}Ca_3(PO_4)_2$	1.5	Could not be precipitated	11,12
β-Tricalcium phosphate (β-TCP)	$\beta\text{-}Ca_3(PO_4)_2$	1.5	Could not be precipitated	12
Amorphous calcium phosphates (ACP)	$Ca_xH_y(PO_4)_z \cdot nH_2O$, $n = 3\text{–}4.5$; 15–20% H_2O	1.2–2.2	~ 5–12	11
Calcium-deficient hydroxyapatite (CDHA or Ca-def HA)	$Ca_{10-x}(HPO_4)_x(PO_4)_{6-x}(OH)_{2-x}$ $(0 < x < 1)$	1.5–1.67	6.5–9.5	11
Hydroxyapatite (HA, HAp or OHAp)	$Ca_{10}(PO_4)_6(OH)_2$	1.67	9.5–12	12
Fluorapatite (FA or FAp)	$Ca_{10}(PO_4)_6F_2$	1.67	7–12	12
Oxyapatite (OA, OAp or OXA)	$Ca_{10}(PO_4)_6O$	1.67	Could not be precipitated	12
Tetracalcium phosphate (TTCP or TetCP), mineral hilgenstockite	$Ca_4(PO_4)_2O$	2.0	Could not be precipitated	11

materials suitable for the development of new drug delivery systems. Controlled drug delivery is the technology by which a drug can be released at a predetermined rate for an extended period into the blood or at target sites.[14] Unlike the traditional oral and intravenous drug delivery methods, where the drug is delivered to both healthy and infected/unhealthy tissues, in controlled local drug delivery, drugs in high concentration can be delivered at the affected sites only. Polymeric drug delivery (organic vesicular delivery) is a well-established procedure in pharmaceutical science. Although these polymeric systems are convenient to deliver a range of drugs including antibiotics, vaccines, steroids, hormones, analgesic, etc., recent advances in nanophase ceramics made drug delivery more effective, solving many challenging medical problems.

The first successful ceramic drug loading and releasing study was performed by Bajpai et al. in 1988 using aluminocalcium phosphorous oxide (ALCAP) scaffolds.[15] The study reports the delivery of several drugs and chemicals such as Danazol and dihydrotestosterone, demonstrating that ALCAP ceramic capsules can release the steroids uninterruptedly for 1 year provided the capsules are impregnated with polylactic acid (PLA). However, while the biocompatibility of those scaffolds had not been confirmed with experimental results, a further study is necessary to establish such long sustainable drug release behavior with other substrates.[16] Pories et al. developed zinc calcium phosphorous (ZCAP) oxide composite ceramic. Use of zinc sulfate calcium phosphate composite in implantable drug delivery systems facilitates the release of zinc in traces and very much effective in wound healing. Although the study was performed prior to 1967, it reported excellent experimental data demonstrating fast healing capacity of ZCAP.[17] Beta-tricalcium phosphate (β-TCP) beads carrying gentamycin and vancomycin have also been used as resorbable bone substitutes in rabbits induced with osteomyelitis. Although gentamycin remained in bone for 10 days, the drug was completely released in 2 days from the implant. On the other hand, the vancomycin released faster, completing within second day. While bacterial concentration on the implant sites proposed an antimicrobial activity, they were not fully sterilized.[18] Guicheux et al. reported the use of human growth hormone (hGH)-loaded macroporous biphasic CaP ceramics as implants in rabbit model. The hGH could be released at the implanted site rapidly during the first 48 h and sustained for another 9 days. The hGH increased

bone ingrowth (+65%) and ceramic resorption (+140%) significantly in comparison with control implants. The biochemical parameters checked in rabbit plasma and urine without any significant differences. The macroporous biphasic CaP revealed as an effective hGH delivery agent for enhanced bone tissue engineering.[19] On the other hand, Nunnery et al. studied the tricalcium phosphate-lysine (TCPL) bioceramic capsules to deliver dehydroepiandrosterone (DHEA, a hormone produced by the adrenals that serves as a precursor for numerous steroid hormones) and estrogen in a sustained manner, demonstrating its proliferative effect on the reproductive organs like ovary, cervix, uterus, and tubes in female rats.[20] However, in male rats, the use of DHEA and DHEA sulfate seemed to show some physiological changes in the vital reproductive organs. DHEA administration inside body system by conventional oral and injection routes faces many challenges such as low sustainability, uncontrolled release, etc. More systematic study is required to overcome such problems.[21] Use of TCPL as a sustained delivery system for releasing medroxyprogesterone acetate (MPA) and estrogen has been demonstrated by Cason et al. The long-term sustained release of MPA and MPA with estrogen and their effect on structural changes in female reproductive system should be studied more critically.[22] The release behavior of cephalexin has also been studied in self-setting bioactive cement based on $CaO–SiO_2–P_2O_5$ glass ceramics.[23] The drug release is seen to continue for 28 days in a simulated body fluid media. The *in vitro* study reveals a very promising material for drug delivery application with its self-setting characteristics for scaffold tissue fixation. However, *in vivo* studies are required for the evaluation of actual physiological performance of these ceramics.

Fabrication of Ceramic Nanoparticles for Site Specific Drug Delivery Applications

Till date, three generations of nanoparticles have been engineered for biomedical applications (Figure 1). The first generation comprised of novel nanomaterials functionalized with simple surface chemistries to assess biocompatibility and subsequent toxic effects. The second generation designed nanomaterials optimized with more complex surface chemistries, which enhance their stability and targeting in biological systems. Presently investigated third generation model augmented their design from stable nanomaterials to 'intelligent' environment-responsive systems with improved targeted compound delivery capacity.[24]

Site-specific delivery of therapeutic compounds with limited effectiveness, poor biodistribution and lack of selectivity are the major limitations for the treatment of many diseases.[25] These limitations or drawbacks can be overcome by designing appropriate drug delivery systems which can protect the drug from rapid degradation or clearance, enhancing drug concentration in desired tissue-specific sites with minimum doses. Cell-specific targeting can be achieved by attaching drugs to exclusively designed carriers of desirable characteristics, tailoring their shape, size, surface property, colloidal stability, along with their surface modification and considering appropriate drug loading mechanism.
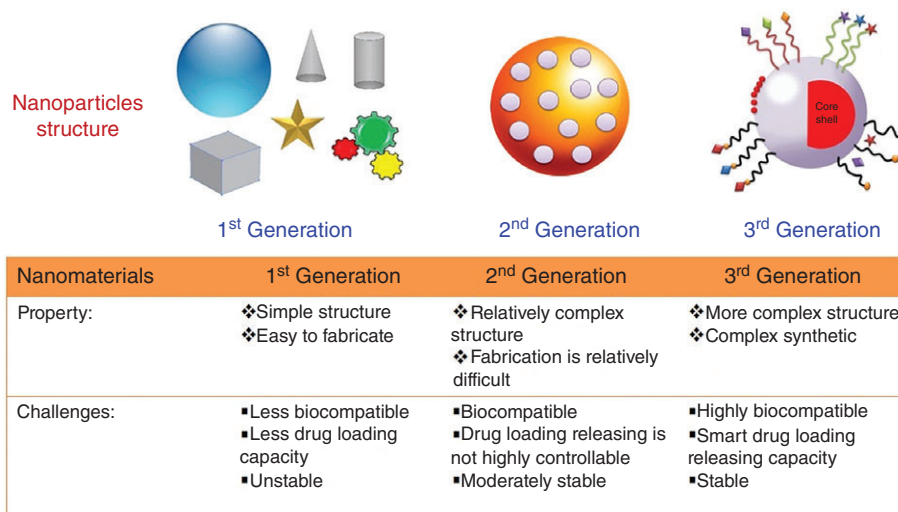

Nanomaterials	1st Generation	2nd Generation	3rd Generation
Property:	❖Simple structure ❖Easy to fabricate	❖Relatively complex structure ❖Fabrication is relatively difficult	❖More complex structure ❖Complex synthetic
Challenges:	▪Less biocompatible ▪Less drug loading capacity ▪Unstable	▪Biocompatible ▪Drug loading releasing is not highly controllable ▪Moderately stable	▪Highly biocompatible ▪Smart drug loading releasing capacity ▪Stable

FIGURE 1 | Three generations of nanoparticles engineered for biomedical applications.

Shape and Size

It has been observed that rod-shaped and nonspherical nanoparticles have a longer blood circulation time compared with spherical particles.[26,27] Moreover, a lower phagocytic activity of macrophages for rod-shaped nanostructures in comparison with spherical nanoparticles has been observed in biological phagocytic studies.[28] On the other hand, spherical nanoparticles have good hydrodynamic flow in comparison with other shapes like rod, plate, flower or wire, etc.[28] Effect of size on particle margination in a flow environment has been studied by Gentile et al.[29] for particles of 50 nm to 10 μm size range, revealing that for particles >500 nm in diameter, the gravitational force causes particle margination towards the wall, whereas for particles <500 nm in diameter, the localization of particles towards the flow chamber wall is a result of Brownian motion.[30] Nanoparticles of sizes smaller than 10 nm are mainly removed by renal clearance, whereas particles bigger than 200 nm are accumulated in the spleen or engulfed by phagocytic cells of the body. Particles with 10–100 nm size range are considered to be optimum as they have longer circulation times in body system, and can easily escape from the reticuloendothelial system of the body. They are also able to penetrate through very small capillaries.[30]

Pore size is an important characteristic of nanomaterials for their applications in catalysis, adsorption, and biomedical (e.g., drug delivery) applications. Among the different porous structures (microporous with pore size <2 nm, mesoporous with pore size 2–50 nm, and macroporous with pore size >50 nm), mesoporous inorganic materials revealed a great promise for biomedical applications such as drug adsorption, storage, and release due to their high pore volume and adequate pore size.[10,26,27,31] They can store a higher amount of therapeutic molecules (Figure 2) in pores. Moreover, mesoporous ceramic structures can be easily functionalized with different chemical ligands, which allow attaching and protecting drug molecules. Frequently, the low density of porous ceramic nanostructures allows them to float in the gastrointestinal tract, prolonging the gastric retention of oral drugs.

Surface Property and Surface Modifications

Preparation of stable colloidal solution is the most essential step for utilizing nanoparticles in drug delivery applications. The surface charge of nanoparticles determines the stability of these colloidal solutions. Nanoparticles having highly positive and negative zeta potentials show higher dispersion
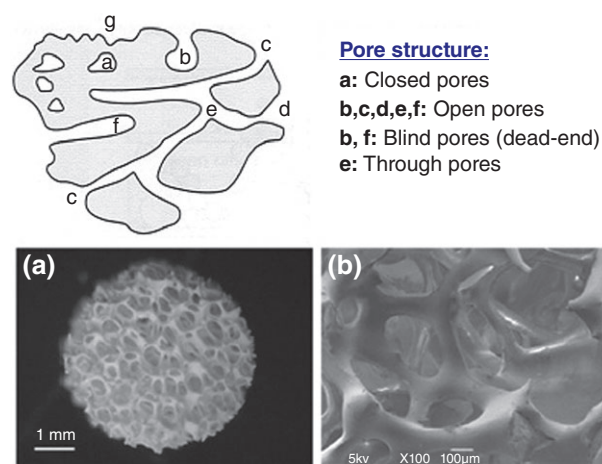

Pore structure:
a: Closed pores
b,c,d,e,f: Open pores
b, f: Blind pores (dead-end)
e: Through pores

FIGURE 2 | Top: Schematic representation of different pore structures. Bottom: Mesoporous hydroxyapatite (HAp) scaffold: (a) stereoscopic and (b) SEM image. (Reprinted with permission from Ref 31. Copyright 2011 Elsevier)

stability, and as a result, do not agglomerate on storage. Surface charge also determines the distribution of nanoparticles in the body system and is an important parameter for the internalization of nanoparticles in target specific cells. Different chemical functional groups possess different affinities to inorganic surfaces; the most well-known example is thiol bonding with gold. This binding is often recognized as 'chemisorption'; sometimes also referred as covalent bond. The exact mechanisms of such bonding are still the subjects of further investigation. Although the point of zero charge (PZC) for HAp is pH = 7.3 ± 0.1, it accumulates positive charge more readily below the PZC than it accumulates negative charge above it.[32] The neutral charge property of HAp at pH = 7.3 is an added advantage for the attachment of ligand molecules on HAp surface at neutral pH, which is physiologically more acceptable for drug delivery system.

Nanoparticles with a hydrophobic surface are easily adsorbed at the protein surface (opsonization) of cellular organelles followed by clearance from the cellular system through macrophages engulfment, resulting a low circulation time in cellular environment.[33] The nanoparticles that are surface-engineered with hydrophilic polymers like polyethylene glycol (stealth particles) containing, for example, hydroxyl or amino functional groups, are able to escape engulfment by the reticuloendothelial cells or circulating macrophages, and show better therapeutic efficiency due to longer retention time in the blood circulating system.[34] Certain ligand molecules, for example, polyethylene glycol (PEG), possess amphiphilic properties, and nanoparticles with those or

other ligand molecules can be soluble in a number of solvents, with intermediate polarity. The strategy for the surface modification of inorganic nanoparticles by biomolecules could be divided into four major classes[35]:

- Ligand-like binding to the surface of the inorganic particle core, commonly by chemisorption. The interaction affinity between ligand and binding part is the result of hydrophobicity, charge, and molecular structure. Different types of binding occur between different ligand and receptors by intermolecular forces, such as ionic bonds, hydrogen bonds and Van der Waals forces.[35]

- Electrostatic adsorption of positively charged biomolecules to negatively charged nanoparticles or *vice versa*. Electrostatic interactions are stronger than covalent bonding.[35]

- Covalent binding by conjugation chemistry, exploiting functional groups on both particle and biomolecules. A covalent bond (molecular bond) is a chemical bond comprises the sharing of electron pairs between atoms. This bond includes different molecular interactions by means of Sigma (σ) bonding, Pi (π) bonding, metal-to-metal bonding, agostic interactions, bent bonds, and three-center two-electron bonds.[36]

- Noncovalent, affinity-based receptor-ligand systems. A noncovalent interaction does not involve electron sharing between molecules. This type of interaction is important to maintain three-dimensional large molecular structures like proteins and nucleic acids.[35]

Surface-modifications of nanoparticles with different functional groups show different surface characteristics, making them appropriate for extensive biomedical application. During the synthesis of nanoparticles, different surface modification reagents (dextran, polyethyleneimine, etc.) are used to control their size, shape, and growth. Surface modification of nanoparticles prevents their agglomeration or cluster formation, improving the colloidal stability of the nanoparticles in different solvents, including body fluids systems of different pH values. Surface modification of nanoparticles also enhances their biocompatibility and bio-functionality, by prohibiting the leakage of toxic ions from them (magnetic nanoparticles) or from the environment to the nanoparticles (free radicals, superoxide, enzymatic activity, etc.). Additionally, surface modification serves as a matrix

for further anchoring functional groups, antibodies, biomarkers, polysaccharides, peptides, etc., to bind or target the nanoparticles to particular cell type or tissue specific regions. Research is under progress to fabricate nanomaterials with enhanced surface properties for biomedical application. Major challenges still present like degradation, clearance from body system due to cell particle interactions, challenging physiological conditions like pH, enzymatic activity, temperature, blood flow, etc., which make difficult to predict the behavior of nanoparticles in biological system.[33–35]

Synthesis of Hydroxyapatite

zAs a biomaterial, the *in vitro* and *in vivo* biological and mechanical properties of HAp are strongly affected by its physical characteristics. Even though a great variety of methods have been tried for the preparation of HAp nanoparticles, only a few of them are acceptable in terms of performance and economic considerations. Main hindrances of most of the used methods rely not only on the diverse precursor, solvent or surfactant materials needed in the synthesis, but also the wide particle size distribution, complicated and expensive processes, major agglomeration and phase impurities, which usually occur in the crystal structures as elucidated in Table 1. A great variety of synthesis methods have been adopted for the fabrication of nanostructured hydroxyapatite (nHAp) worldwide. Efforts have been made to control their geometry, crystallinity, size, stoichiometry, and degree of particle agglomeration (for different applications) by employing new routes or through modification of pre-existing synthesis methods. Nano- and micron-sized HAp particles of distinct morphologies have been synthesized in large scale with tailored composition, reproducible size, structure, etc. Recently, environmentally friendly synthetic methodologies, including biomimetic synthesis, molten-salt synthesis, hydrothermal processing, and template synthesis, have been instigated as viable techniques for the synthesis of a range of bioceramics. Nanometric HAp particles could be prepared by a variety of wet-chemical techniques such as sol–gel, chemical precipitation, hydrothermal, polyol, micro-emulsion, and sonochemical; employing dry techniques such as solid state method and mechanochemical synthesis; high-temperature synthesis such as combustion, spray pyrolysis, and thermal decomposition; and from various biogenic sources.[9] The production of synthetic ceramic HAp biomaterials can be classified as:

- Wet-chemical synthesis (precipitation, hydro-thermal, hydrolysis and sol–gel techniques).
- Dry-chemical synthesis (solid-state reactions, mechanochemical synthesis).
- High temperature reactions (combustion, spray pyrolysis, thermal decomposition).
- From bio-resources (biological origin) such as (1) Animal sources: bovine, sheep, pigs, goats, etc., bones and teeth; (2) Marine sources: fish scale, bones, red algae, corals, sea shells, sea urchins, etc.; (3) Plant sources: papaya leaves, calendula flowers, bamboo, potato orange banana peels, grapes, etc. (Figure 3).

Utilization of different synthesis methods produces HAp nanostructures of different sizes and shapes as can be seen in Table 2.

Structure of Hydroxyapatite

The inorganic mineral phase of bones consists of small crystallites of ion-substituted HAp, which is formed by the replacement of a fraction of carbonate groups of carbonate apatite by phosphates and/or hydroxyl groups in the structure.[95] The unit cell of HAp (synthetic or natural origin) has a hexagonal crystal structure, with space group $P6_3/m$ and lattice constants a and c equal to 0.942 and 0.688 nm, respectively. The crystal structures of apatite have
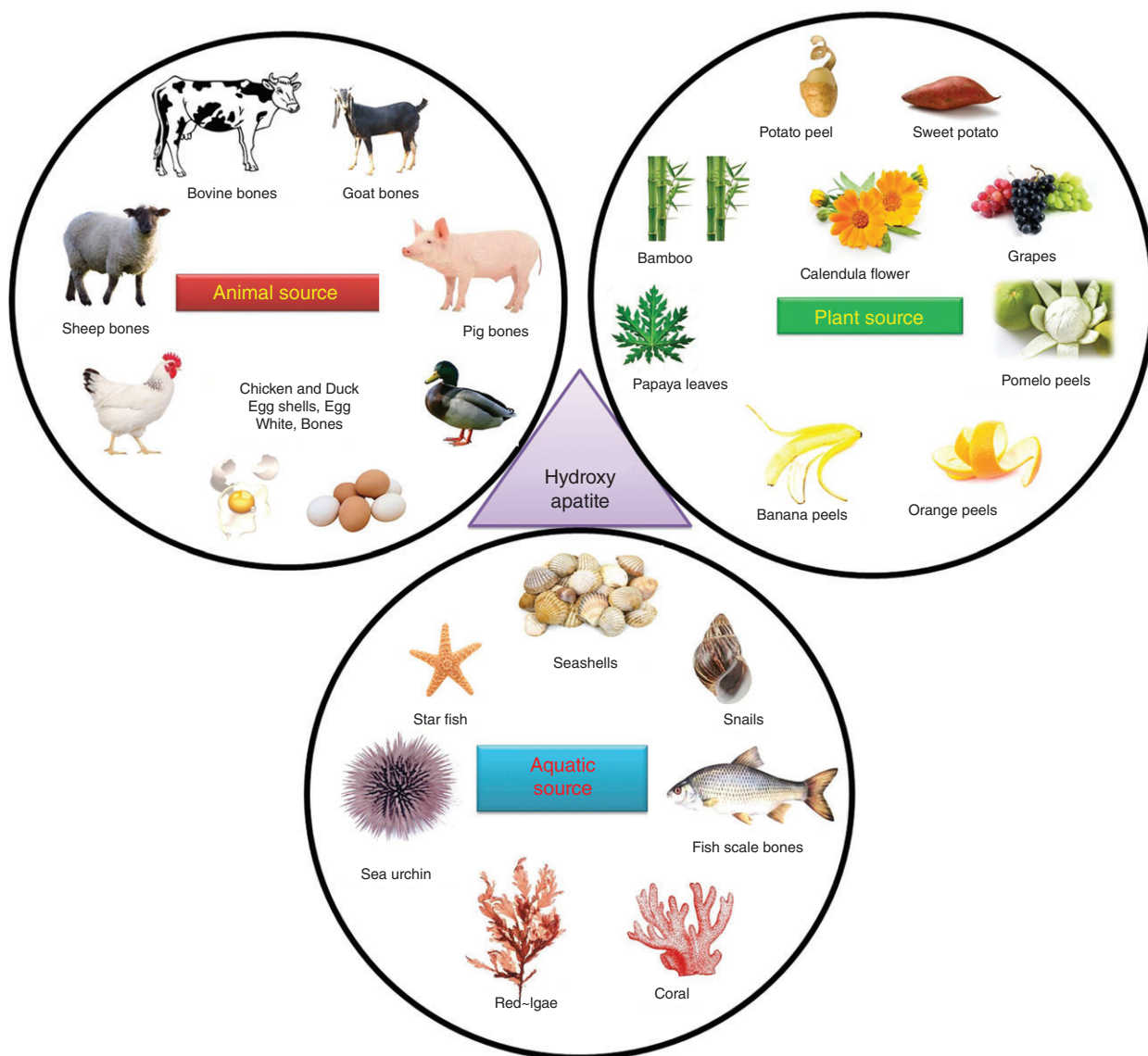

FIGURE 3 | Bio-sources for hydroxyapatite (HAp) synthesis: Animal (top left), plant (top right) and aquatic (bottom).

TABLE 2 | Hydroxyapatite (Hap) Nanostructures of Different Sizes and Shapes Produced Using Different Synthesis Routes

Synthesis Route	Advantages	Morphology and Size	Ref.
Wet-chemical synthesis			
Co-precipitation	Simplest and most efficient chemical method. Synthesis at room temperature. Particle size can easily be controlled by adjusting pH and ionic strength of reaction media. Nanostructures of wide range of size and morphology.	Irregular, sphere, rod, needle, tube, fiber, filament, wire, whisker, strip, platelet, flower. Size range: 3 nm–1000 μm.	10,37–40
Sol–gel synthesis	Molecular-level mixing of reactants improves the chemical homogeneity of synthesized pure and hybrid nanostructures at low temperature.	Irregular, sphere, rod, needle, tube, filament, whisker, platelet. Size range: 3 nm–1000 μm.	10,41–45
Hydrothermal synthesis	Enhanced solubility of precursors. Controlled growth dynamics.	Irregular, sphere, rod, needle, tube, fiber, wire, whisker, feathery structures. Size range: 3 nm–1000 μm.	10,46–50
Micro-emulsions	Controlling better particle size, restrict hard agglomeration.	Irregular, sphere, rod, tube, flower. Size range: 5 nm–8 μm.	10,51–55
Polyol	Nonagglomeration, High boiling point of polyols used as a solvent as well as a reducing agent.	Irregular, leaf, flake, plate, whisker, nanorods. Size range: 5 nm–80 μm.	10,48,56,57
Sono-chemical	Monodispersed nanoparticles of different shapes could be produced.	Irregular, sphere, filament, rod, tube. Size range: 5 nm–1000 μm.	10,58–61
High temperature synthesis			
Thermal decomposition	Good size control, narrow size variation and good crystallinity.	Irregular, flake, plate, sheet, formless. Size range: 5 nm–200 μm.	10,62–65
Pyrolysis	Rod-like nanoparticles and single phase with high crystallinity and good stoichiometry.	Nanorods embedded to micron form. Size range: 10 nm–1000 μm.	10,66–69
Combustion	Quickly procedure, high purity, single step operation.	Sphere, oval, ball, irregular spherical. Size range: 5 nm–200 μm.	10,70–74
DRY SYNTHESIS			
Solid state	Well crystallized structure.	Irregular, filament, rod, needle, whisker. Size range: 5 nm–1000 μm.	10,75–79
Mechano-chemical	No calcination is required.	Irregular, sphere, rod, needle, whisker. Size range: 5 nm–200 μm.	10,80–84
Synthesis from bio sources			
Bio sources [Animal, Plant and Aquatic]	To produce HAp ceramics from various natural materials such as bone waste, eggshells, marine organisms, naturally derived biomolecules and bio membranes. This is an eco-friendly approach to convert waste materials to wealth.	A diverse structure could be obtained. The different shapes include sphere, irregular, flakes, plate, rod, tubular structure, etc. Size range: 10 nm–2000 μm.	65,85–94

been studied in details by Naray-Szabo[96] which was confirmed further by Hendricks et al.[97] The proposed structure was further refined by Posner et al.[98] The HAp lattice consists of Ca^{2+}, PO_4^{3-} and OH^- ions distributed over two mirror symmetric halves of the unit cell (Figure 4).[99,100] In a single cell unit of HAp, there are 14 calcium ions; of which six are located within the unit cell, and the remaining eight peripheral ions are shared by adjacent unit cells. Among the 10 PO_4^{3-} groups of a unit cell, two remain inside and eight at the periphery. All the eight OH^- groups remain at the edge of unit cell, shared by 4 unit cells each. Therefore, on average, each unit cell of HAp

contains 10 calcium ions, 6 phosphate ions, and 2 hydroxyl ions.

Applications of Hydroxyapatite

HAp has been widely used to treat bone and periodontal defects,[101] alveolar ridge,[102] as dental materials,[103] middle ear implants,[104] tissue engineering systems[105] and bioactive coatings on metallic osseous implants,[106] due to its adequate mechanical properties and the similar composition to bone and teeth minerals.[107] Recent studies also suggest that HAp particles inhibit the growth of many types of cancer cells.[108,109]
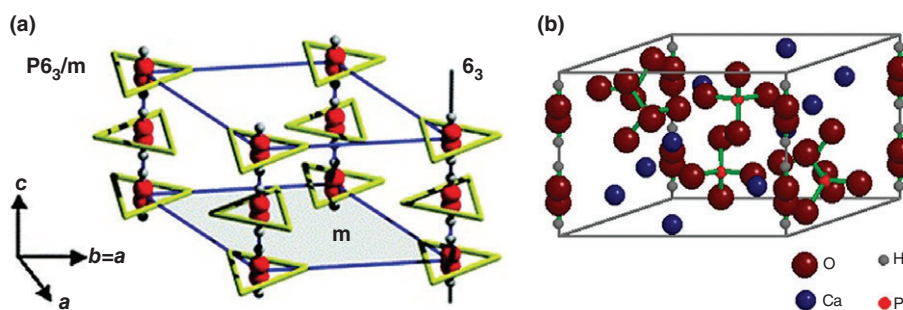
FIGURE 4 | Molecular structure of hydroxyapatite (HAp): (a) computational modeled hexagonal crystal structure with P63 symmetry. Calcium ions are at the vertices of the triangles around each hydroxyl group (red). (Reprinted with permission from Ref 99. Copyright 2010 Royal Society of Chemistry. (b) Unit cell perspective. (Reprinted with permission from Ref 100. Copyright 2007 Elsevier)

The general importance of HAp and its derivatives has also led to numerous nonmedical industrial and technological applications, such as chromatography adsorbents for purification and separation of proteins and nucleic acids,[110] catalysts,[111,112] host materials for lasers,[113] fluorescence materials,[114] ion conductors,[115] and gas sensors.[116] In addition, HAp presents very convenient qualities for water treatment processes,[117] and remediation of heavy metal contaminated soils.[118]

HAp of various morphologies and surface properties have also been investigated as drug carriers for the delivery of a variety of pharmaceutical molecules, because of their tailorable size, structural advantages, highly active surface, unique physical and chemical properties, ease of modification, biocompatibility, nontoxic, and noninflammatory properties.[119–121]

Biocompatibility is an important factor to understand the host response with implants and biomaterials. On tissue engineering aspect, biocompatibility is defined as the ability of materials to locally trigger and guide normal wound healing, reconstruction, and tissue integration. *In vitro* biocompatibility is performed with specific cell lines (bone: osteoblast, cartilage: chondrocyte, liver: hepatocyte, etc.) to determine its interaction. For the biocompatibility evaluation of HAp materials, MG63 osteoblast cell lines are used. While HAp is a well-studied biocompatible material, its surface provides a suitable matrix for attachment of cells, showing no toxic effect, allowing cells to proliferate over it. The bone and scaffold implant interface revealed the presence of HAp as one of the important factor in the bonding zone. *In vivo* studies revealed primary dissolution of ions from the surface of implanted HAp, followed by ion exchange and structural rearrangement at the ceramic–tissue interface. Enhancement of cellular activity causes cell attachment, proliferation, and differentiation, which ultimately forms an extracellular matrix.[122]

'Nontoxic' materials are considered to be nondangerous or nondestructive to living beings. Nontoxic is also a relative term, which is considered by many factors like quantity, environment or condition and target specific. Considering these factors in mind, if any material in minute quantity shows detrimental (lethal) effect, then its toxicity is to be considered as higher. HAp, a constituent of calcium and phosphorous, has been well-studied for its toxicity under different conditions and with different cell lines, as well as in animal models. There exists no report on its toxic behavior in normal conditions. The formula of HAp is $Ca_{10}(PO_4)_6(OH)_2$, consisting of Ca^{2+}, PO_4^{3-} ions and it is very stable material in physiological environment. During implant-tissue interaction in physiological system, the release of Ca^{2+}, PO_4^{3-} ions favors for bone cell formation and does not show any toxic effect.[123]

'Inflammation' is the result of complex biological protective response involving immune cells, blood vessels, and molecular mediators. The function of inflammation is to eliminate the early cause of cell injury, clear out necrotic cells and damaged tissues due to an inflammatory process, and to initiate tissue repair. The classical signs of inflammation are heat, pain, redness, swelling, and loss of function.[6–12,119–121] The implantation study of HAp scaffold does not show any inflammatory effect due to its bioactive and nontoxic properties.[86]

HYDROXYAPATITE AS A DRUG CARRIER

A variety of ceramic drug delivery systems have been utilized to carry different types of drugs such as amino acids, steroids, hormones,[124,125] proteins,[126]

vaccines,[127] phenolics, acetylsalicylic acid, genes, antigens, enzymes, antibiotics[128–130] and anti-cancer drugs.[131] HAp has a low solubility in physiological condition and it could be used as a carrier for the local delivery of drugs both by surgical placement and injection. Three important forms of drug delivery by HAp are: (1) drugs conjugated/loaded with implanted HAp scaffolds, (2) porous HAp/nHAp granular particles, and (3) polymer coated HAp/-nHAp particles. Use of HAp as drug carrier agent has several advantages:

- HAp nanoparticles usually have longer biodegradation times, a property crucial to diffusion-controlled drug release kinetics. Slowly degradable—or even close to nondegradable—ceramic matrices can retain drugs for longer times after administration. The controlled localized drug delivery by HAp minimizes the toxicity to other organs by minimizing the drug concentration in the blood. The drug concentration could be controlled in a way that it neither reaches the toxic level nor falls below the minimum effective level, and also circumvents repeated dosage of drugs.[124,125,127–130]

- The concentration of the loaded drug over porous HAp surface depends upon the penetration behavior of the drug molecules through the micropores, the rate of penetration, and the pharmacokinetic profile of the drug. Since engineered HAp contains microporous structure and has excellent biological response to the physiological condition, it can ensure slow release of the drug.[22–24,119–127,130]

- HAp can functionalized/bonded with both positively and negatively charged molecules by simple adsorption.[131]

- HAp does not swell or change porosity, and is relatively stable under the variation of solution pH and temperature. The small swelling ratios of ceramics prevent the release of a burst of drugs—a problem commonly seen in hydrogels, such as poly (2-hydroxyethyl methacrylate) (pHEMA) drug-delivery system.[130,132]

- Synthetic HAp nanoparticles can posse the same chemistry, crystalline structure and size as of the constituents of targeted tissues (e.g., various types of CaP in bone or teeth).[1,10,39–43,85,101–107]

- Through doping, HAp could be tailored as nanoparticles with favorable electrical (e.g., ferroelectric and dielectric), mechanical

(e.g., piezoelectric, ultrahigh hardness, etc.), magnetic (e.g., superparamagnetic) and optical (e.g., photothermal effects, electroluminescence, etc.) properties which is hardly seen in polymeric nanoparticles.[113,114,126,130,132]

Mechanism of Drugs Attachment over Hydroxyapatite

Mechanisms of biomolecule immobilization over the surface of HAp particles or implant materials are discussed in very few articles. To provide a controlled and sustainable drug loading impact on cells, it seems beneficial to develop biomaterial surfaces with covalently immobilized ligands, which provide controlled release of proteins or drugs.[133]

A number of approaches have been developed for the conjugation of therapeutic agents or targeting ligands on the surface of nanoparticles (Figure 5). They can be classified in two major groups. One is the conjugation of drug by means of cleavable covalent linkages and the other is attachment through physical interactions.

Covalent linkage strategies involve linking therapeutic agent or targeting molecules directly with, for example, amino or hydroxyl functional groups present on the surface of polymer-coated nanoparticles. Alternatively, linker groups such as iodoacetyls, maleimides, and the bifunctional linker pyridyl disulfide may be used to attach the drug to the surface of the particles. This approach not only leads to an
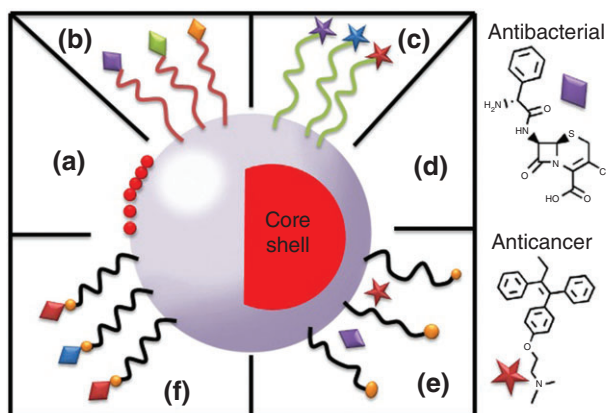
A: Coating of HAp surface with nanoparticles
B: Physical Interaction of Antibiotics
C: Physical Interaction of Anticancer Drugs
D: Core shell magnetic HAp
E: Non covalent attachment
F: Covalent attachment of Drugs

FIGURE 5 | Schematic presentation of drug conjugation processes over hydroxyapatite (HAp) nanoparticles.

enhancement of the loading capacity but also results in more specific linkages, protecting the drug's functionality and hence increasing its efficiency. Another advantage of using linkers is they provide milder reaction conditions for attachment, which is favorable for the drug molecules such as therapeutic peptides, proteins, and polymers to be protected from harsh chemical environments.

Physical interactions such as electrostatic, hydrophobic/hydrophilic and affinity ones can also lead to coupling of drug molecules with the surfaces of nanoparticles. Polyethyleneimine (PEI), a cationic polymer, interacts electrostatically with negatively charged nanoparticles. The nonspecific cell uptake and severe toxicity of PEI conjugated nanoparticles are still a big challenge for its utilization in nanomedicine. To overcome such constraints, compatible ligand-mediated modification of PEI is necessary to reduce its cytotoxicity and enhance cellular uptake.[134]

Similarly, dextran-coated nanoparticles functionalized with negatively charged functional groups can be coupled with peptide oligomers via electrostatic interactions. The limitation associated with dextran coating includes pulmonary edema, acute renal failure, cerebral edema.[135]

Due to hydrophobic interactions, lipophilic drugs can easily be attached to nanoparticles covered with hydrophobic polymers. In this case, the degradation of hydrophobic polymer coating causes the release of therapeutic drugs. Affinity interactions, such as streptavidinbiotin and biotinylated interactions, can also be utilized for bioconjugation of therapeutic agents with HAp nanoparticles. Unlike electrostatic and hydrophobic interactions, affinity interactions offer the most stable noncovalent linkages, which are relatively unaffected by environmental conditions, such as changes in pH and ionic strength of the medium.

Grafting hexamethylene di-isocyanate to HAp surface has also been used to immobilize drugs over HAp surfaces. The reaction procedure for grafting hexamethylene di-isocyanate requires multistep chemical reactions in presence of catalyst and inhibitors.[136] Introduction of amine groups on HAp surface through aminosilanization helps to immobilize therapeutic molecules.[137] HAp particles modified with aminopropyl-triethoxysilane have been evaluated to be nontoxic to a variety of cells in biocompatibility screening. Hydrolysation of silane molecules has serious effects on cell morphology, which in high concentration causes cell injury leading to cell death. The use of aminosilanes has always favored over vinyl silane or methacryloxy silane coatings due to the improvement of hydrophilicity, which causes enhanced cell adhesion on the surface.[137] Silanized HAp has also been used for the immobilization of RGD (Arginylglycylaspartic acid) peptides with enhanced cell adhesion and differentiation. RGD, a tri-amino acid sequence, is the most commonly studied adhesive peptide in the biomaterials field. RGD sequence can bind to multiple integrin species and minimizes the risk of immune reactivity or pathogen transfer. In spite of these advantages, the RGD interaction with integrin binding protein is very broad. As a result, the chances of nonspecific binding of target molecules are very high, because blood and other body fluids contain high amount of integrin binding proteins.[138,139] Other approaches for surface functionalization utilize compounds comprising strong adsorptive binding to HAp surfaces, such as phosphates, amino acids. The crystallinity of HAp nanoparticle influences the surface activity and solubility.[140] Poly-glutamate motifs,[141] and polyelectrolytes like poly acids,[142] have been utilized to create a platform for covalent binding of drug molecules with RGD coated nHAp structure. In Table 3, a few examples of drug conjugation with HAp utilizing different approaches are presented.

HAp Nanoparticles as Drug Carriers for Healing Bone Related Disorders

Application of HAp as a drug-carrying medium/vehicle is mainly focused on treating hard tissue diseases, especially bones and teeth. It is a proven efficient inorganic drug delivery agent for the treatment of chronic osteomyelitis and bone cancer. On the other hand, HAp is useful to deliver drugs of low bone penetration and short biological half-life.[149,150] Poly-methyl-methacrylate (PMMA) beads have been utilized initially to treat infectious bone diseases. However, they had to be removed surgically as they are nonbiodegradable. Use of resorbable biomaterials like collagen, fibrinogen, and PLA are seen to be ineffective drug carries, as they do not replace bone grafting.[151,152] On the other hand, treatments of bacteria infected bone diseases such as osteomyelitis and osteoarticular infections are highly complicated, which involve operative debridement, and removal of all foreign bodies through follow-up antibiotic therapies.[153] The blood circulation in these infected sites is limited and hence the antibiotic distribution is poor. Therefore, growth factors and antimicrobials should be supplied to the osseous sites by site-specific drug delivery.[154,155]

On the other hand, nano- and micrometric HAp of different morphologies (spherical, irregular,

TABLE 3 | A Few Examples of Effective Conjugation of Therapeutic Drugs with Hydroxyapatite (Hap) through Different Approaches

Drug Conjugation Approach	Conjugated Drug	Performance	Ref.
Cleavable covalent linkage	Doxorubicin (DOX)	Mesoporous HAp acts as an excellent carrier for DOX molecules with a loading efficiency of $\approx$ 93%, which is much higher than that of the conventional HAp particles. Variation of pH of the release medium (PBS) from 7.4 to 5.5 increases the drug release from 10% to about 70%.	143
	Raloxifene	Raloxifene used in osteoporosis therapy, inhibits osteoclast. Forms a covalent bond with nHAp-based biomaterial by interfacing with (3-aminopropyl)-Triethoxysilane (nHAp coating material). No drug loading or releasing kinetics were studied. By employing FTIR, the functional groups were studied and possible mechanism of raloxifene conjugation on HAp surface has been discussed. HAp contains hydroxyl groups which may react with the 3-aminopropyl-triethoxy silane and subsequently condenses the amino group of the silane with the Ketone group of raloxifene.	144
	Ofloxacin	β-cyclodextrin (β-CD) has covalent interaction with HAp. Coupling agents are used to improve the drug (ofloxacin) loading capacity and for sustained release. The adsorption capacity of ofloxacin on β-CD-grafted HAp (β-CD-g-HAp) composite was found to be about 30 mg/g at 37 °C in 24 h. The release of ofloxacin from β-CD -gHAp slows down to 28% and 21% in pH 2.0 and 7.4, respectively, within 2 h.	145
Attachment through physical interaction	Ibuprofen	Ibuprofen exists in dimeric form both in solid and liquid state. Ibuprofen—nHAp complex formation occurs most likely through the dissociation of Ibuprofen dimer into monomeric species. Hydrogen bonding of the hydroxyl group of Ibuprofen to the hydroxyl group of the apatite, together with the interaction of the ibuprofen carbonyl group to HAp Ca center.	146
	Sodium ampicillin	HAp contains negatively charged hydroxyl groups (OH^-), which are the potential bridging agents to sodium ampicillin, which has positively charged groups such as amine group (NH_3^+), sodium ions (Na^+) and some hydrogen ions (H^+). Three stage release kinetics, independent of loading concentration (1, 5 and 10 mg of ampicillin/ml) has been observed. The first stage, characterized by a fast release (first 2 min), followed by the slower second stage, which lasts approximately 12 min. In the final stage, a residual volume of sodium ampicillin is released, which lasts until the finish of sodium ampicillin in the samples ($\sim$30 min.).	147
	Vancomycin	Vancomycin was loaded with HAp and PCL coated HAp scaffold via immersion-adsorption method. The drug release studied for short (1 h) and prolonged (72 h) time durations. Compared to the abrupt initial burst (as high as $\sim$70–80% release) in uncoated HAp samples, the PCL coated HAp showed much lower initial burst ($\sim$44%). The study revealed $\sim$90% release of the drug within 24 h for the pristine HAp sample.	148

whisker, rods, etc.) have been used to fabricate porous scaffolds to deliver drugs in traumatized or post-operative bone tissues. For example, Son et al. reported ionic immobilization of dexamethasone (DEX)-loaded poly(lactic-*co*-glycolic acid) (PLGA) microspheres over HAp scaffold surfaces. In that study, HAp scaffolds with interconnected porosity were prepared followed by immobilization of DEX-loaded and FITC-loaded PLGA microspheres in a three step process. Primarily, PLGA microsphere surfaces were treated with radiofrequency plasma in an oxygen-filled chamber, followed by the second step of dispersing the oxygen plasma-treated PLGA microspheres in positively charged PEI solution and lyophilization. The final step involved DEX-loaded PLGA microspheres immobilization on the negatively charged HAp scaffold surfaces (Figures 6 and 7).

In vitro drug release from the encapsulated microspheres was evaluated prior to their implantation in defective femurs of beagle dogs. The release profile of DEX in phosphate-buffered saline (PBS, pH = 7.4) at 37 °C, over a 28 days immersion study indicated an initial burst release, followed by a sustained release. The immobilized microspheres showed
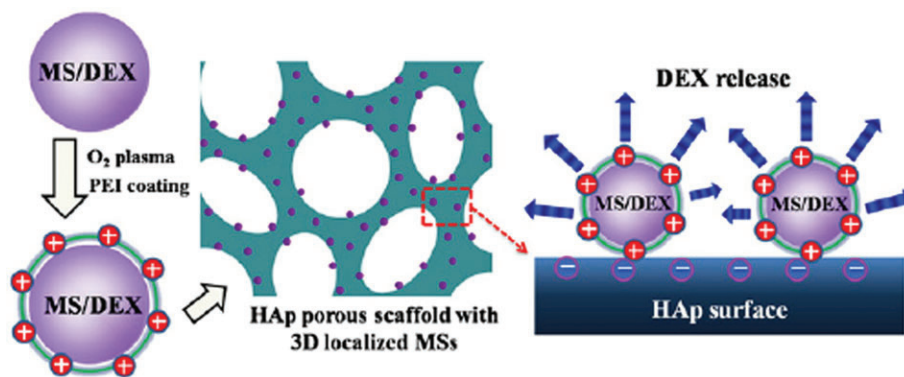
FIGURE 6 | Schematic diagram of the porous hydroxyapatite (HAp) scaffold containing Dex-loaded PLGA microspheres. PLGA microspheres were pre-coated with PEI molecules. The counter charge of the microsphere and HAp surfaces permitted fabrication of the system via electrostatic interactions. (Reprinted with permission from Ref 31. Copyright 2011 Elsevier)

an early burst of approximately 35% of the total DEX loaded at day 2, followed by a sustained release of DEX for the remaining study period. *In vivo* evaluations of DEX-loaded PLGA microsphere-immobilized HAp porous scaffolds were also performed. After 10 weeks of *in vivo* implantation study, micro-computed tomography (micro-CT) analysis revealed new dense cortical bone formation at DEX-loaded HAp scaffolds implantation region. Whereas, the traumatized regions which were either unfilled or filled with DEX-free HAp scaffolds slowed healing with less dense bone formation.

Among other important drug delivery studies of HAp, the standout might be of Shinto et al., who studied gentamicin-, cefoperazone- and flomoxef-loaded cylindrical HAp blocks of different sizes for osteomyelitis against staphylococci.[156] While gentamicin sulfate elution from the HAp blocks could be detected until 90 days of loading, cefoperazone showed similar release pattern, detectable until 50 days. On the other hand, flomoxef showed most rapid release from HAp blocks, lasting until 25 days. Itokazu et al. used arbekacin antibiotic-loaded HAp blocks for the treatment of osteomyelitis in rats.[157] The HAp blocks used in this experiment were of $2 \times 2 \times 3$ mm dimension, with 50% porosity and 50–300 μm pore diameter, where about 0.84 mg of arbekacin could be introduced to each of them. The release of loaded antibiotics from the HAp blocks has seen to be very slow and stable. About 0.5 μg/L arbekacin was retained in the HAp blocks after 40 days of study.

Among other bone bonding motifs,[158] bisphosphonates are a class of substances characterized by a high affinity for bone and HAp.[159] The capacity of bisphosphonates to accumulate in bones is a
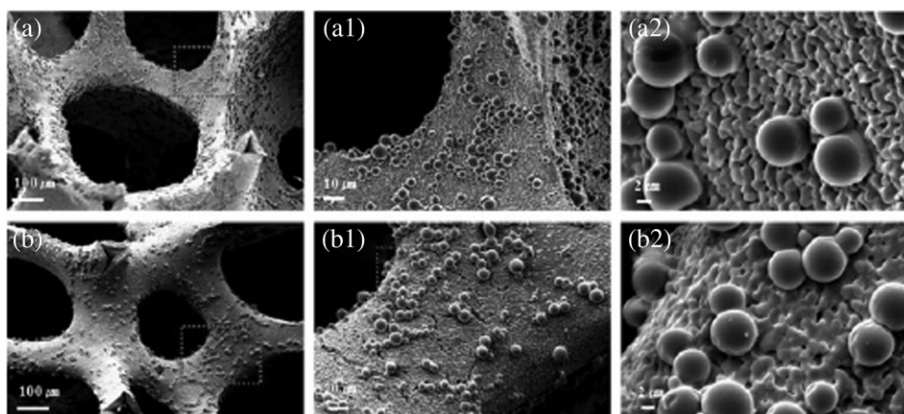

FIGURE 7 | SEM images of DEX-loaded PLGA microspheres immobilized onto hydroxyapatite (HAp) scaffold. (a, a1, a2) HAp scaffold after shaking for 4 h with water-dispersed control PLGA microspheres; (b, b1, b2) HAp scaffold after shaking for 4 h with water-dispersed PEI coated PLGA microspheres. (Reprinted with permission from Ref 31. Copyright 2011 Elsevier)

consequence of their high affinity to HAp due to bi- or tri-dentate interactions, depending on the structure of the respective derivative.[160] The influence of the chemical structure of bisphosphonate derivatives on their bone-binding affinity and the growth of HAp crystals have been studied by several researchers.[161] For example, Ong et al. have synthesized HAp nanoparticles of various sizes (40–200 nm) and demonstrated that they can be stably loaded with drugs (radioisotopes) by exploiting the high-affinity HAp–(poly) phosphonate interaction.[162] According to their study, clinically available phosphonates, clodronate, and Tc-99 m-methylene-diphosphonate (Tc-99 m-MDP) could be efficiently loaded onto HAp nanoparticles within 15 min. Utilizing noninvasive micro single photon emission computed tomography (microSPECT), they could monitor the biodistribution of Tc-99 m-MDP loaded radiolabeled HAp nanoparticles in mice. Imaging and dosimetry studies indicated that HAp nanoparticles, regardless of size, were quickly taken up by Kupffer cells in the liver after systemic administration into mice. Clodronate loaded HAp nanoparticles remained biologically active and could result in selective depletion of Kupffer cells. However, the use of bisphosphonates in drug targeting to bone is more common due to their adequate pharmacokinetic properties. Especially they are ideal candidates for targeting bone and calcified tissues, as has been demonstrated by Hirabayashi and Fujisaki through bisphosphonate-conjugated proteins. [163]

Nanostructured HAp as Drug Carrier

Since last two decades and a half, researchers have given a considerable effort for applying HAp nanostructures as a suitable drug carrier agent.[164] To mention a few, Cellet et al. synthesized HAp nanowhiskers to load terbinafine, an antifungal drug, to deliver in colon.[13] With a BET estimated specific surface area of 67 m^2/g, the synthesized nanowhiskers [crystallite size of 8.41 nm along (211), and 23.7 nm along (002)] could adsorb about 40.63 mg of terbinafine/g of HAp. The HAp nanostructures have seen to be excellent drug delivery vehicles, releasing about 90% drug in simulated gastric fluid, and about 70% in simulated intestinal fluid in 30 h.

Yu et al.[165] fabricated antimicrobial composites to protect prosthesis from deep infection using irregular shaped HAp nanoparticles of 30–40 nm size as carriers of vancomycin hydrochloride (VAN). For that, they incorporated VAN loaded HAp nanoparticles into a sticky matrix of oxidation sodium alginate and gelatin, which acted as a good adhesive to the

prosthesis. The VAN loading capacity of HAp nanoparticles was seen to be about 956 μg per 100 mg HAp nanoparticles. Although the authors have not studied the drug release behavior of the composite, the VAN release pattern from the bare HAp nanoparticles was seen to have two strides. During the initial 24 h, there was a burst release of VAN, releasing 61% of total amount of loaded VAN, and during later 375 h, there was a slow release of VAN entrapped in HAp nanoparticles porous channels. The results clearly demonstrate the possibility of using HAp nanoparticles for controlled sustained drug delivery.

On the other hand, Lian et al.[166] fabricated vancomycin-loaded nHAp/collagen/PLA bone graft substitute with infection inhibition property for repairing large size bone damages. Although the shape and size of the used HAp nanoparticles were not reported, the composite graft revealed a typical porous structure with a porosity of about 80% and compressive strength of 1.52 MPa. The release kinetics of VAN from the composite graft was studied *in vitro* using phosphate buffer solution, revealing about 98% release of the loaded drug in 4 weeks. The composite graft was seen to have a high level of bacterial inhibition ratio (> 99%), with good adhesion to the trauma site and without any inflammation responses in subcutaneous implantation.

Finally, hollow HAp nanoparticles such as hollow spheres and nanotubes of 36–60 nm in diameter have been utilized for VAN storage and its controlled release by Ye et al.[167] demonstrating their high drug holding and pH-controlled drug release capacities. Although it is not easy to fabricate hollow HAp structures at nanoscale, they reported an innovative polymeric micelle-templating method for fabricating hollow nanospheres and nanotubes of HAp. Utilizing the complex solubility behavior of polyethylene oxide (PEO) and polypropylene oxide (PPO) below and above their critical micellar temperature and dehydration kinetics of PEO at cloud temperature, they fabricated Tween 60 conjugated PEO-PPO-PEO triblock copolymer templates to produce hollow HAp nanospheres (Figure 8). On the other hand, by utilizing citric acid as co-surfactant in the same process, they succeeded to assemble those spherical polymeric templates to linear assemblies, which could be used to fabricate HAp nanotubes (Figure 8). It has been demonstrated that these hollow nanospheres (drug holding efficiency ~19.06%) and nanotubes (drug holding efficiency ~31.82%) have much higher VAN holding capacity than their solid counterparts such as nanoparticles of similar sizes (drug holding
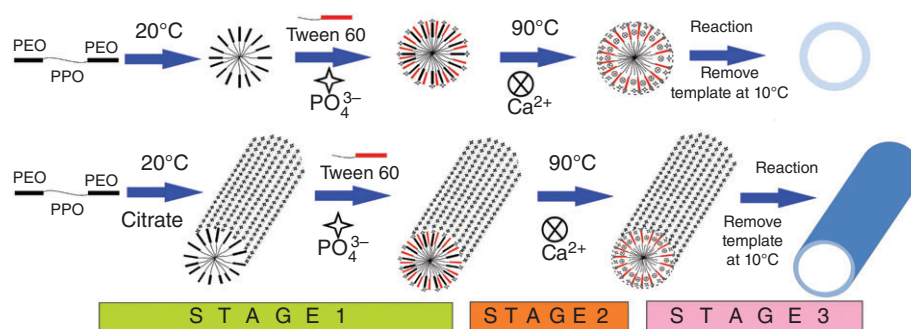
FIGURE 8 | Schematic representation of hollow hydroxyapatite (HAp) nanoparticles fabrication from P123 and Tween-60 core–shell structured micelles templates. (Recreated with permission from Ref 167. Copyright 2010 Elsevier)

efficiency ~2.25%). The drug holding capacity of the HAp nanotubes could be increased further by functionalizing them by cationic polyelectrolyte poly(dimethyldiallyl ammonium) chloride, PDDA, which forms electrostatic charge complex with the negatively charged carboxyl ion of the co-surfactant citric acid. The VAN release behavior of these polymer-functionalized nanotubes strongly depends on the strength of interaction (hydrogen bonding) between the VAN and carboxylic group of citric acid and the pH-dependent protonation of the carboxylic group (Figure 9).

HAp nanoparticles have also been used as carriers for anticancer drugs. The specific properties of drugs and morphology of HAp nanoparticles were seen to affect the adsorption and desorption kinetics of drug molecules. The negatively charged alendronate and the positively charged cisplatin were strongly adsorbed, while the neutral di(ethyle-nediamineplatinum) medronate (DPM) complex showed a lower affinity towards the negatively charged surface of HAp nanoparticles. While adsorption of cisplatin was found to be favored at needle-shaped HAp surface, plate-shaped HAp surface favored alendronate adsorption. However, the release rate of neutral DPM was seemed to be higher than that of charged alendronate and cisplatin. While neutral DPM released at a faster rate from needle-shaped HAp surface than plate-shaped surfaces, both the charged drugs revealed similar release rates from both types of HAp nanoparticles.[168]

The studies performed by Venkatasubbu et al. confirmed the effectiveness of PEG functionalized HAp nanoparticles as a drug carrier.[169] Anticancer drug paclitaxel could be effectively attached to the surface of folic acid modified PEG-functionalized HAp surface. The drug loaded polymer functionalized nanoparticles revealed usual release pattern (initial burst release followed by

prolonged sustained release), releasing 100% of the drug in 50 h. The initial burst release has been associated with the facile detachment of the drug molecules from the surface of the HAp nanoparticles. Doxorubicin (DOX) intercalated nHAp has been utilized as drug-delivery system into adult female Swiss Albino rat model for treating liver cancer.[170]

Using 'opposite ion core-shell' inorganic template strategy, for the first time, Ma et al. fabricated hollow ellipsoidal capsule shape HAp and calcium silicate (CaSiO$_3$) nanostructures for drug delivery applications.[171] For the development of core HAp or CaSiO$_3$ structures, they used nanostructured (400–600 nm diameter and 600–900 nm length) core of CaCO$_3$ as templates (Figure 10). CaCO$_3$ cores were synthesized via wet-chemical reaction of Ca(CH$_3$COO)$_2$ and NaHCO$_3$ at room temperature, where Ca(CH$_3$COO)$_2$ was used as Ca^{2+} source.
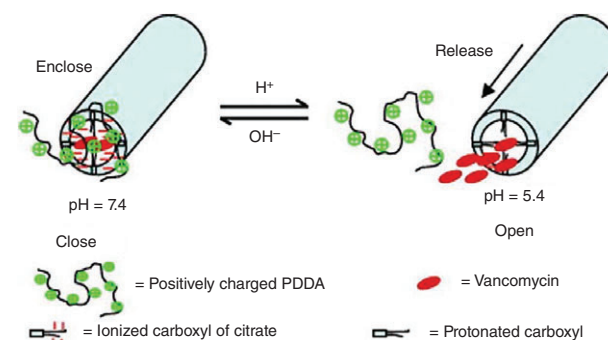

FIGURE 9 | Schematic representation of pH-responsive drug carrier, based on the interaction between negatively charged carboxyl groups of citrate upon hollow hydroxyapatite (HAp) nanorods surfaces and positively charged poly dimethyldiallyl ammonium (PDDA) molecules. The interaction formed the gates to open or close to store or release vancomycin from the hollow nanorods, as controlled by environment pH. (Reprinted with permission from Ref 167. Copyright 2010 Elsevier)
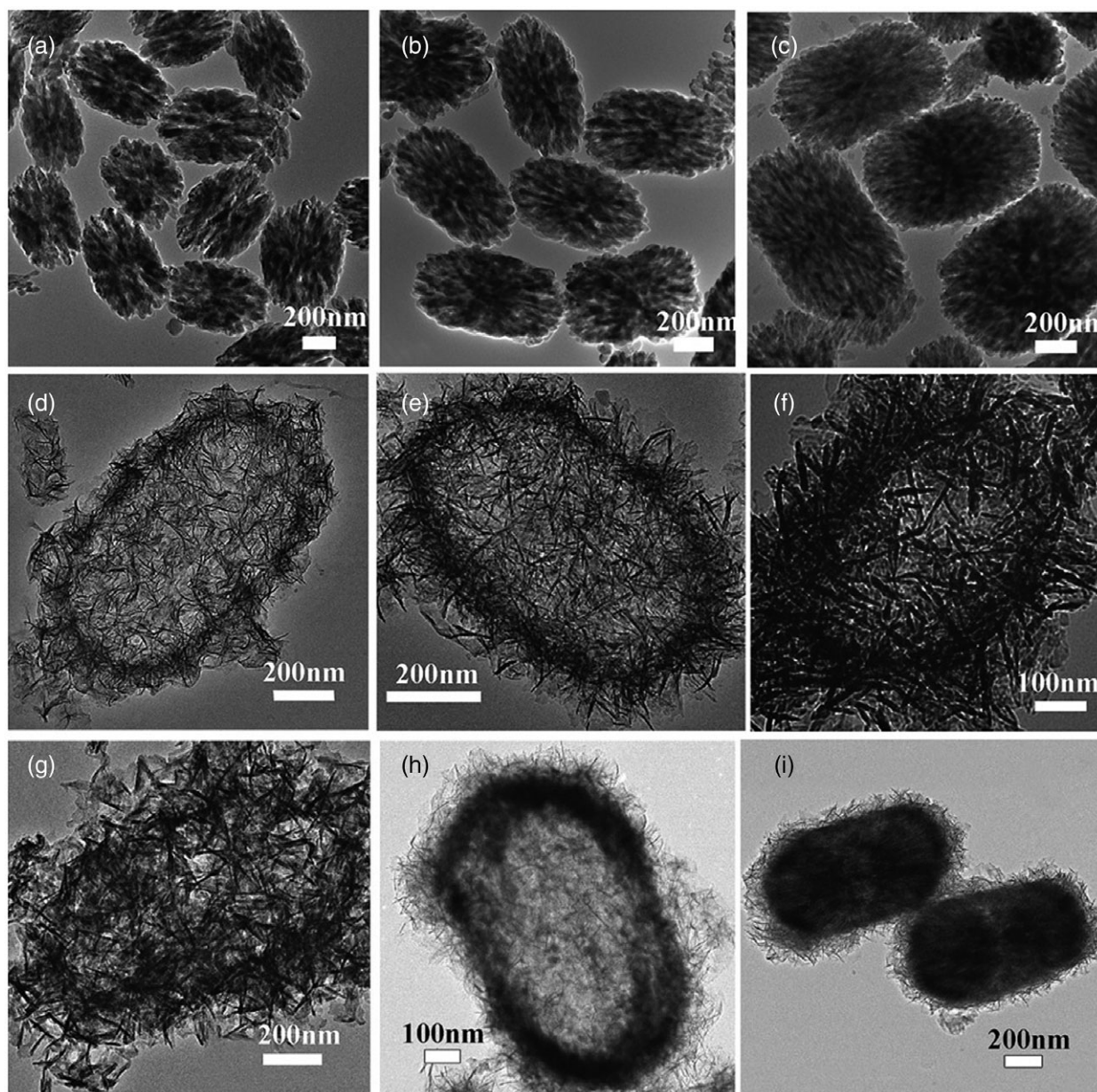
FIGURE 10 | TEM micrographs of (a)–(c) $CaCO_3$ cores with different sizes (d)–(i) HAp hollow ellipsoidal capsules nanostructures with different shell thicknesses prepared by using the $CaCO_3$ cores. (Reprinted with permission from Ref 171. Copyright 2008 Royal Society of Chemistry)

Next, either PO_4^{3-} or SiO_3^{2-} source was added to form HAp or $CaSiO_3$ shells, respectively, on the surface of $CaCO_3$ cores. A follow-up treatment with dilute acetic acid and calcination at 900°C could completely remove the $CaCO_3$ cores to make the capsules hollow. The synthesized hollow HAp nanocapsules were studied for drug loading and release, with a model drug ibuprofen (IBU), which could be stored at 459.5 mg/g of the nanostructures. The drug release pattern revealed a very slow and sustained release of IBU through diffusion for 100 h. Loaded IBU did not release completely from nanostructures because of the formation of hydrogen bonds between –COOH groups of IBU and –OH groups of hollow HAp nanocapsules, which retarded or held back the drug release.

Li et al.[172] synthesized mesoporous HAp (MHAp) nanoparticles using Pluronic F127 block copolymer as a template. To obtained disulfide functionalized MHAp (S-S-MHAp) a series of chemical reactions were performed to develop first the NH_2-MHAp and then COOH-MHAp. The developed COOH-MHAp

co-dissolved with *N*-hydroxysuccinimide and 1-[3-(dimethylamino) propyl]-3-ethylcarbodiimide hydrochloride in phosphate buffer solution with the further addition of cystaminedihydrochloride to develop S-S-MHAp. Fluorescein isothiocyanate (FITC) was utilized as both model drug and site marker for intracellular tracing of MHAp. The S-S-MHAp/FITC was further covalently coupled with carboxyl groups of collagen and amino groups of S-S-MHAp. This constructed the redox-responsive MHAp nanoreservoirs end-capped with collagen. Finally, lactose acid (LA) was added to the collagen-capped MHAp solution to develop cell-specific targeting complex moiety of LA-Col-S-S-MHAp/FITC (Figure 11(a)).

In drug loading and releasing assays, LA-Col-S-S-MHAp has been utilized as a FITC carrier complex. Endcapping efficiency and release behavior of LA-Col-S-S-MHAp/FITC have been followed by UV–vis fluorescence spectroscopy. To explore the controlled release behavior, dithiothreitol (DTT) was used as an external stimulus to trigger the redox-responsive release of FITC. About 20% of FITC was released from LA-Col-S-S-MHAp within 10 h without using DTT; which indicates a good end-capping efficiency (Figure 11(b), i-a). On the addition of DTT, the LA-Col-S-S-MHAp/FITC system exhibited 80% release within 10 h; which concludes the rapid response to DTT due to the breakage of disulfide linkages between collagen and MHAp (Figure 11(b), i-c). Col/MHAp-FITC exhibited around 80% FITC leaching after 20 h due to the inferior end-capping efficiency of physically coated Col/MHAp compared to the Col-S-S-MHAp disulfide linkages system (Figure 11(a), i-b). To investigate the rapid redox response of LA-Col-S-S-MHAp to an external stimulus, DTT was added to the solution after 5 h cultivation of LA-Col-S-S-MHAp/FITC in PBS buffer solution. The result showed that without DTT about 10% of FITC was released after the first 5 h, whereas, on co-addition of DTT addition, 70% FITC was released after a subsequent 5 h (Figure 11(b), ii). The disulfide linkages between collagen and MHAp of LA-Col-S-S-MHAp/FITC nanocomposite have good end-capping efficiency, which promotes a rapid redox-response to DTT under physiological conditions to deliver or release drugs.[172]

A recent work of Li et al.,[173] demonstrated the synthesis of core-shell mesoporous nano-hydroxyapatite (MHAPNs) by templating method, using Pluronic F127 as block copolymer template, and polyacrylic acid (PAA) as the shell. The construction of drug loading systems (DOX@PAA–MHAPNs) was performed through several chemical reactions; first with 3-aminopropyltriethoxysilane

(ARTS) to obtained NH2-MHAPNs, followed by *N,N*-dimethylformamide (DMF) and PAA (Mw = 3000) to obtain PAA–MHAPNs. Finally, DOX was added to PAA–MHAPNs nanocomposite to obtain DOX@PAA–MHAPNs (Figure 12(a)). *In vitro* controlled drug release behaviors of DOX@-PAA–MHAPNs and DOX@MHAPNs were studied in PBS buffered solutions at pH 7.4 (mimicking the physiological pH in normal tissues and blood), 6.5 (mimicking tumor extracellular environment), and 5.0 (mimicking subcellular endosomes). As can be seen in Figure 12(b) i), the drug release behavior of DOX@PAA–MHAPNs could be regulated by the solution pH. The drug release rate from the DOX@-PAA–MHAPNs system after 24 h in pH 7.4 was about 15%. Whereas, the release amount of DOX increased up to 48% and 72% after 24 h, on decreasing the pH of the solution to 6.5 and 5.0, respectively (Figure 12(b), i). Such pH dependent DOX release behavior of the DOX@PAA–MHAPNs system has been attributed to the protonization of PAA at lower pH environment, which lead to a dimension of electrostatic interactions between PAA and DOX. However, the drug release behavior of the DOX@MHAPNs system (Figure 12(b), ii) was seen to be less sensitive to the solution pH.

Insufficient or uncontrolled intracellular drug release from nanoparticles always limits the amount of drugs that actually reach to target sites, which severely hampers the efficacy of treatment and induces toxic side effects inside body system. To overcome the challenges, till date, various nanoparticles have been used as drug delivery agent. Among them, HAp nanoparticles have a promising future to be an ideal nanostructured material as a therapeutic agent.

HAp Nanoparticles as Protein Carriers

One of the positive aspects of HAp as a drug carrier molecule is its strong ability to adsorb proteins on surface.[110,126,133] Researchers have studied the adsorption behavior of different proteins such as cytochrome *c* (Cyt *c*), hemoglobin, and bovine serum albumin (BSA) over HAp surfaces.[174–176] Liu et al. synthesized calcium deficient nHAp by *in situ* and *ex situ* schemes with BSA loading on their surface. The study revealed the release behavior of BSA from the nHAp carrier at different pH environments (7.5, 8.5, and 9.5). The uptake amount of BSA by the synthesized nHAp decreases with increasing pH value. At pH 7.5, the amount of incorporated protein was about 17.5%, which is 75% higher than normal BSA loading. The BSA release profile of nHAp shows
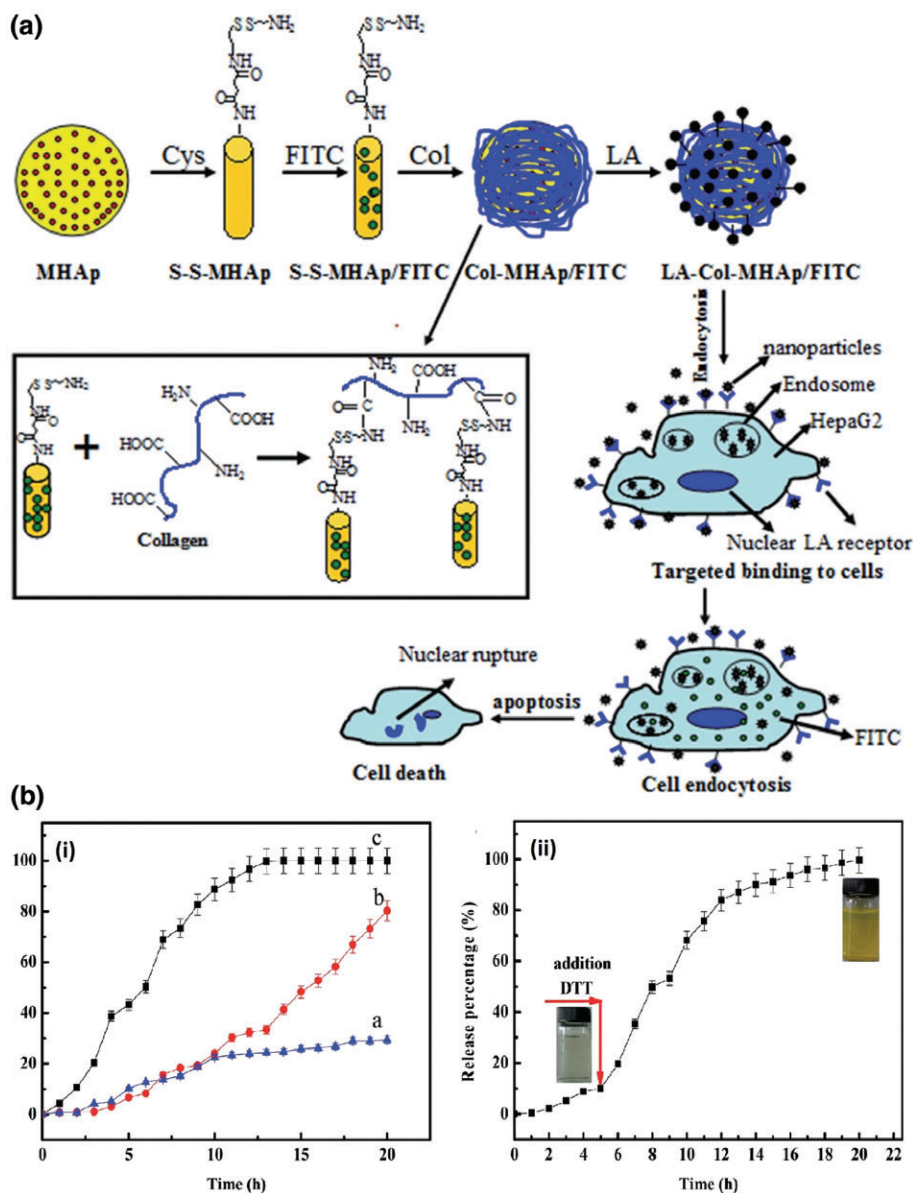
FIGURE 11 | (a) Schematic illustration of redox-responsive system based on collagen capped MHAp (mesoporous hydroxyapatite) for cell-targeted drug delivery (b) Cumulative release profiles of FITC from LA-Col-S-S-MHAp with/without DTT solution: (i) controlled release of FITC from LA-Col-S-SMHAp (a and b without DTT, c with DTT) and the Col/MHAp system (b); (ii) delayed release of FITC from LA-Col-S-S-MHAp by addition of DTT solution after incubation for 5 h. (Reprinted with permission from Ref 172. Copyright 2014 Royal Society of Chemistry)

two stages, the initial fast released by desorption followed by a slow release due to crystal dissolution.[176]

Xu et al. studied the interactions of HAp nanoparticles with Cyt c and hemoglobin and their influence on the development of zebrafish, a model animal, for developmental biology. Their experimental results indicate the interactions of the two functional proteins with HAp nanoparticles are electrostatic attraction and hydrogen (N-H- - -O and O-H- - -O) bonding. Interactions of HAp nanoparticles

with peptide chains result in twisting the proteins, causing the breakage of hydrogen bonds; changing the secondary conformation of proteins to sheet-like conformation. Furthermore, HAp nanoparticles aggregate to bigger particles around the membrane proteins, causing a mild toxicity to the development of zebrafish embryos.[177]

For the application in guided tissue regeneration (GTR), it is very important to develop resorbable materials with sufficient mechanical strength. Talal
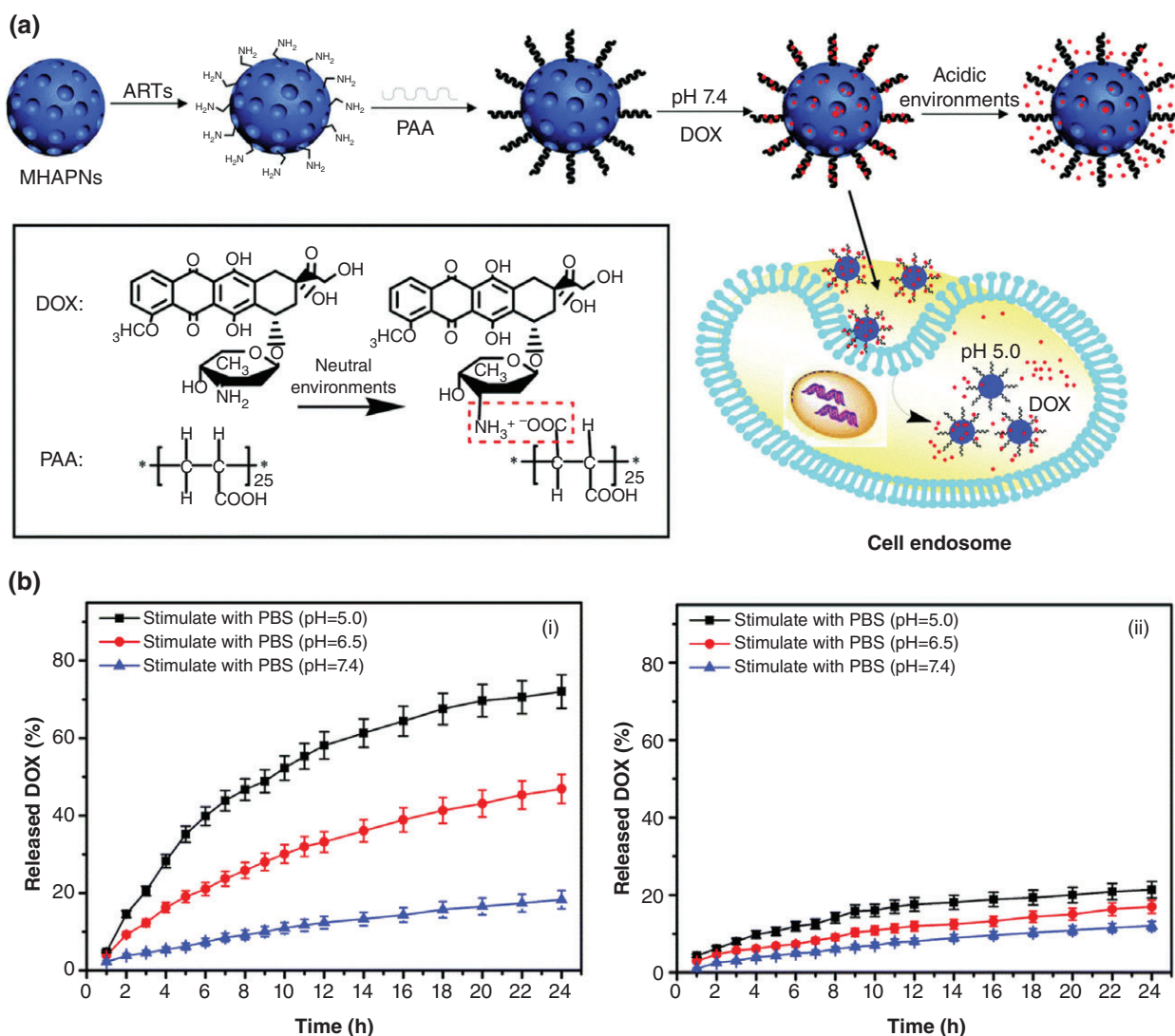
FIGURE 12 | (a) Schematic illustration of the preparation of DOX@PAA–MHAPNs and the intracellular pH-responsive drug delivery system (b) Cumulative release profiles of DOX from (i) DOX@PAA–MHAPNs and (ii) DOX@MHAPNs at different pH values. (Reprinted with permission from Ref 173. Copyright 2016 Royal Society of Chemistry)

et al. developed a HAp nanoparticles/polylactide (PLA) composite membrane and studied its interaction kinetics with proteins. HAp nanoparticles incorporated PLA membrane was seen to adsorb BSA very fast (within 5 min of treatment), with about eightfold increase in BSA protein holding with respect to PLA membrane without HAp nanoparticles. The diffusion of BSA through HAp nanoparticles/PLA composite membrane increased with the increase of HAp nanoparticle content. The diffusion of BSA in PBS from the developed PLA membrane after 24 h was only 3.64 ± 1.01 µg/mL. Whereas, PLA membranes with 25% and 75% HAp nanoparticles showed 44.99 ± 35.61 µg/mL and 153.12 ± 65.57 µg/mL of protein diffusion, respectively. These composite membranes are therapeutically useful as delivery systems for controlled release of proteins.[178]

Use of Doped HAp Nanostructures for Real-Time Monitoring of Drug Release

Although pure HAp is a nonluminescent material, luminescent properties can be induced in it by incorporating rare-earth ions, especially the ions of lanthanide groups such as Eu^{3+} (europium), Gd^{3+} (gadolinium), and Sr^{2+} (strontium) for real-time monitoring of drug release. On the other hand, lanthanide ions such as Eu^{3+} and Gd^{3+} functionally mimic Ca^{2+} (calcium) ions can affect the bone remodeling cycle, which makes lanthanide-doped HAp as a potential

material for the treatment of bone density disorders such as osteoporosis.[179] Another possibility of inducing luminescent properties in HAp is through conjugation or adsorption of fluorescein ($C_{20}H_{12}O_5$)-type organic fluorescent materials at its surface.[180,181] These lanthanum ion doped or fluorescent conjugated HAp nanostructures can be utilized for monitoring drug loading and release characteristics of these nano-structured vehicles, as well as for tracking drug distribution at the treated sites. Furthermore, as the incorporation of lanthanide ions induces magnetic properties on HAp nanostructures, there is a good possibility for using them as biomarkers. In fact, Zhang et al. utilized Sr.-doped mesoporous HAp nanorods for *in vitro* monitoring of loading and releasing kinetics of model drug IBU, by monitoring the intensity of the characteristic blue emission of Sr^{2+} ions around 432 nm. In addition, Chen et al.[182] utilized multifunctional Eu^{3+}/Gd^{3+} dual-doped HAp nanorods for the whole body *in vivo* imaging in nude mice through computed tomography for monitoring the release and distribution of IBU at the injected sites (Figure 13). On the other hand, a considerable enhancement of the drug loading capacity of HAp nanorods (from 653.5 to 841.4 mg/g) has been observed due to the enhancement of the specific surface area and zeta potential of lanthanide-doped HAp nanostructure surfaces.

Due to isotropic electronic ground state $^8S_{7/2}$ and half-filled *f*-orbitals, both the trivalent europium and gadolinium ions posse high magnetic moment and proton relaxation (both longitudinal and transversal) at low magnetic fields. Such electronic

structures of these rare earth ions make the rare earth doped HAp nanostructures ideal biomarkers for computer tomography (CT) scan and magnetic resonance imaging (MRI). These multifunctional nanostructures hold a promising future to enhance clinical therapeutic efficacy in bio-imaging and drug delivery contexts.

Magnetic HAp-mediated Drug Delivery

Since the introduction of the concept of using magnetism in medicine by Freeman et al.[183] in the 1960s, a vast amount of research work has been performed in this area, leading to the design of several magnetic particles and vectors. The idea of targeted drug delivery and targeted drug therapy is to transport a drug directly to the affected sites under various conditions and thereby treating them skillfully without any side effect on the affected sites of the body. Most types of magnetic HAp nanoparticles are based on iron oxides. Investigations have also been performed (Figure 14) on magnetic HAp nanoparticles based on other dopants. The magnetic HAp nanoparticles are broadly categorized in eight different categories such as (1) Fe-doped, (2) Fe and Pt co-doped, (3) iron oxide doped, (4) Cobalt-ferrite doped, (5) Mn and Fe doped, (6) Nd and Gd co-doped, (7) ^{153}Sm and Gd incorporated, and (8) iron oxide, Fe and Cu doped HAp nanoparticles.[184]

Tran et al. reported increased osteoblast functions in the presence of HAp-coated iron oxide nanoparticles.[185] Their hydrothermally synthesized HAp coated rod-shaped Fe_3O_4 nanostructures (60 nm
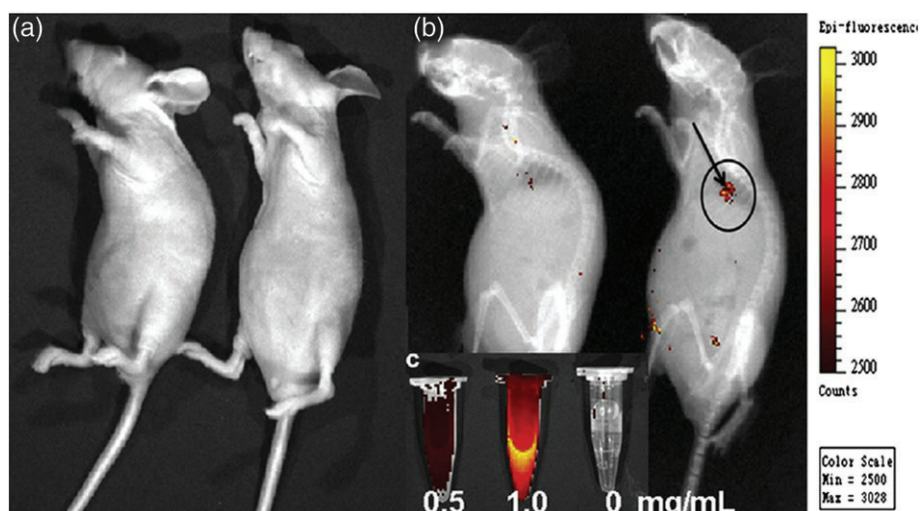

FIGURE 13 | *In vivo* PL imaging of the mice after subcutaneous injection without (a) and with (b) Eu^{3+}/Gd^{3+}-HAp (Eu^{3+}: Gd^{3+} = 1:2) nanorods. (c) PL emission images of Eu^{3+}/Gd^{3+}-HAp nanorods at different concentrations. The excitation wavelength was 430 nm. (Reprinted with permission from Ref 182. Copyright 2011 Elsevier)

long, 20 nm wide) had saturation magnetization (M_s) of ~35 emu/g which revealed good osteoblast activity when cultured with osteoblast cells. However, the composite nanostructures were not been used for drug delivery application. Hou et al.[108] synthesized magnetic HAp (mHAp) nanoparticles by co-precipitation method and reported their application in animal model (mouse) to treat tumor by magnetic hyperthermia. The mice, which were only injected with mHAp and had been treated inside the magnetic field showed a dramatic reduction of tumor volume in 15 days long experimental observation period (Figure 14, ii). Whereas, the mice injected with mHAp did not show any reduction effect over tumor when they were not under a magnetic field (Figure 14, iii). The blood test results of liver and kidney functions of the experimental mice possess important information regarding biocompatibility of the HAp and mHAp nanoparticles. The normal blood urea nitrogen (BUN) and creatinine level in the experimental mice suggest normal kidney functions, whereas, the elevated alanine aminotransferase (ALT) and aspartate aminotransferase (AST) levels suggest abnormal liver functions due to the metabolism of HAp and mHAp through liver. The increased ALT and AST levels are not fatal because all the mice survived well during the experimental study. All the animals under study revealed normal alkaline phosphatase (ALP) levels, which confirm the normal bone metabolism even after the exposure of the nanomaterials in the body system.

Guo et al. utilized magnetic, mesoporous carbonated HAp microspheres as drug delivery systems for loading and releasing VAN, although the saturation magnetization of their composite nanostructures was very low (M_s ~3.98 emu g^{-1}). About 35.1 wt% of vancomycin could be loaded per gram of the developed carrier, and about 67.5% of it was released after 20 h.[186]

On the other hand, Gu et al. have developed mesoporous Fe_3O_4/HAp nanocomposite with large surface area, high pore volume, and good magnetic separability.[187] They utilized the Fe_3O_4/HAp composite with about 16.20 emu/g saturation magnetization for DOX loading and releasing, observing about 0.102 g of DOX loading per gram of the composite; while its release kinetics revealed a faster early stage release and slower prolonged release (until 100 h), depending on the pH of the release medium. The slow, steady, prolonged and safe release behavior of the composite demonstrates its utility as an ideal material for targeted drug delivery.

The versatile intrinsic properties of magnetic HAp nanoparticles enable their use in numerous therapeutic applications in the field of diagnostics and therapeutics. More specifically, the use of magnetic HAp nanoparticles with their unique guiding capabilities and negligible side effects, are excellent drug delivery agents, not only for cancer therapy but also in treatment of other ailments.

In this review, we analyzed the experimental results of different research groups on the drug

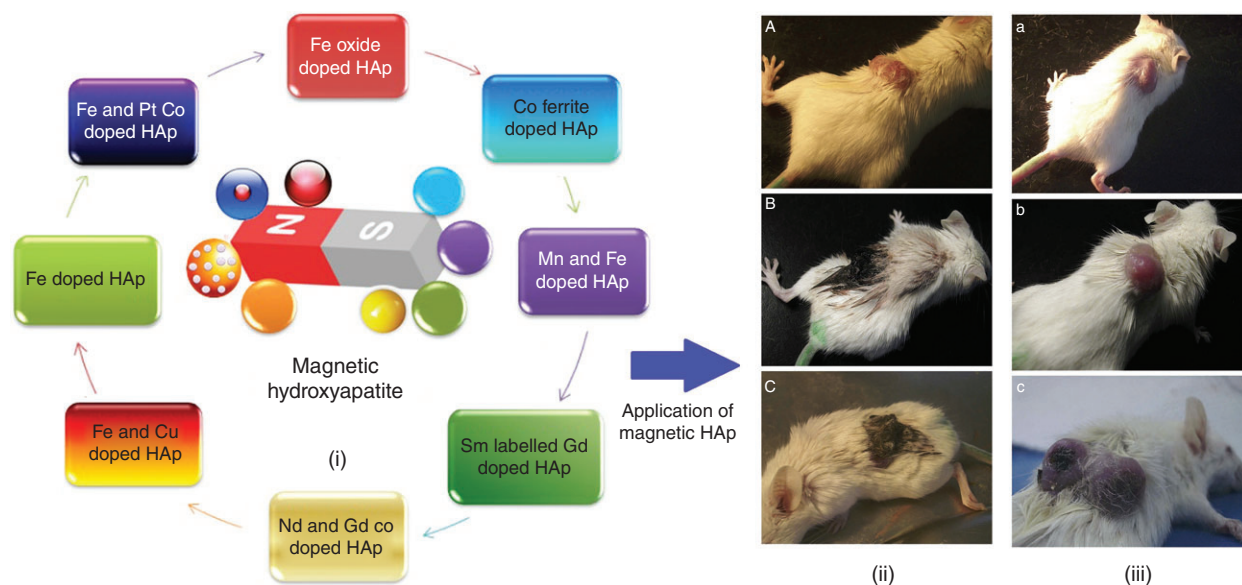**FIGURE 14** | (i). Magnetic hydroxyapatite (mHAp) nanoparticles based on different dopants. (ii) The clinical photographs of the tumor (mHAp with magnetic field). The tumor in day 1 (A), day 5 (B), and day 14 (C). (iii) The clinical photographs of the tumor (mHAp without magnetic field). The tumor in day 1 (a), day 5 (b), and day 14 (c). (Reprinted with permission from Ref 108. Copyright 2009 Elsevier)

loading and releasing behaviors of HAp nanostructures, along with their utilization for bioimaging (Table 4). Although most of the drug delivery studies on HAp nanostructures have been performed utilizing these nanostructures in scaffolds, and on bone-related corrective surgery, the results demonstrate that the drug-loaded nHAp has very different drug uptake and release patterns over a prolonged period. Depending on the shape, size, composition, and porosity of the nHAp based carrier, very different drug uptake and release kinetics can be revealed for a particular drug molecule. Similarly, different drug molecules show varying drug uptake and release behaviors for the HAp nanostructure of particular shape and size. However, it is clear that HAp nanostructures are well efficient to carry a broad range of molecular structures including biological molecules such as proteins, enzymes, nucleic acids, etc.

The studies performed so far revealed that tailored HAp nanostructures can deliver therapeutic molecules to specific areas of the body efficiently with release control, and reduced side effects. HAp nanostructures of <100 nm dimension have enhanced drug uptake and better-controlled release behaviors than bulk HAp. Although a vast amount of experimental work has been published in the literature, they do not lead us to conclude if the morphology or size of HAp nanostructures plays any significant role on the efficiency of these nanostructures for drug delivery.

TABLE 4 | Hydroxyapatite (HAp) Nanostructures Used for Drug Delivery and Imaging Application

Drugs with HAp	Application	Nature of HAp	Ref.
Paclitaxel, Cis-diamminedichloroplatinum (II), Di(ethylenediamineplatinum) medronate, Methotrexate	Anticancer drug delivery	Nanoparticles, Scaffold or block of nanoparticles of HAp	170,188–191
Eu^{3+} and Gd^{3+} doped	Tri-modal contrast for MRI, X-ray and NIR fluorescence	Nanoparticles of 30 nm average size	179
Fe^{2+} and Pt^{2+} doped	Lung cancer and hyperthermia	Pt and Fe doped nanoparticles	192
Arbekacin sulfate, Vancomycin, Ceftriaxone, Gentamicin, Cefoperazone sodium, Flomoxef sodium, Hydrocortisone,	Antibiotic drug delivery	Nanoparticles, Scaffold or block of HAp	163,166,191–194
Iron doped Poly lactic acid (PLA)	MRI contrast agent, scaffold	HAp nanoparticles	195
Iron (Fe^{3+} and Fe^{2+}) doped	Targeted drug delivery, Imaging	Needle shape, superparamagnetic	196
Fe_3O_4, Fe and Cu doped composite	Targeted drug delivery and MRI	Porous nanoparticles	197
Iron (Fe^{3+}) doped	Nano-probes for drug releasing	Rod shaped nanoparticles of 75 nm average size	196
Tb^{3+}/Gd^{3+} dual-doped	Bimodal imaging applications	Spherical (40–100 nm)	198
Functionalized with luminescent and magnetic Na(Y/Gd)F4:Yb^{3+}, Er^{3+}	Drug delivery and MRI bimodal contrast agents	HAp nanoparticles	199
Dual doped with Ho(III) ion and Fluorescein isothiocyanate labeled	*in vitro* cell imaging and as T2 MRI contrast agent	Magnetic and luminescent	200
Dye (FITC) functionalized	Cellular imaging, drug delivery	Needle shape nanoparticles (50–100 nm)	201
Luminescent mesoporous Eu-doped	Luminescent drug carrier and bioimaging probes	Rod shaped, 20–40 nm wide and 100–200 nm length	202
Ln (Eu^{3+}, Tb^{3+}) doped	Luminescent drug carriers and bioimaging probes	Rod shaped nanoparticles	203
$CePO_4$:Tb doped	Redox luminescent switch and bioimaging probes	Needle shaped, 50–100 nm length, 5–10 nm wide	204
Cr^{3+} doped	Bioimaging/biosensing	Nanoparticle, 40–100 nm	205

However, the composition and porosity do have significant effects on the drug loading (though adsorption, conjugation or attachment) capacity of nHAp and HAp composites.

The positive and most promising aspects of HAp nanostructures as drug delivery agent are their nontoxic and bioactive behaviors. Moreover, HAp nanostructures of tailored composition and morphology can be fabricated through simple synthesis techniques. HAp nanostructures of high active surface allow a broad range of therapeutic molecules to be adsorbed, adhere or attached on their surfaces. All these characteristics make HAp nanostructures most promising carrier agent among the common bioceramics. With the progress of science and technology, we gain more knowledge on the disease pathology and cellular defense mechanisms, which help us to develop specific drugs. To improve the specificity and strength of these newly developed drugs, advanced drug delivery systems must be instigated. Considering

TABLE 5 | Patents Related with Nanostructured Hydroxyapatite for Medicinal Application

Sl.	Patents	Application Potentials
1	US20170027989 A1 (February 2, 2017) Rajan V. Vembu	Compositions and methods for the prevention and treatment of metabolic diseases (hydroxyapatite nano-fibers composite)
2	WO2016202100 A1 (December 22, 2016) Zhang Li et al.	Polyether ether ketone/nano hydroxyapatite dental implant and manufacturing method thereof
3	IN201401516-I1 (December 11, 2015), Ahmad F J et al.	Nano-conjugate composition useful for regulated release of antiresorptive agent
4	JP2015223259-A (December 14, 2015), Furusono T et al.	Hydroxyapatite-derived particles used in deodorizer and dental filler
5	CN104857567-A (August 26, 2015), Hu Y et al.	Calcium alginate/hydroxyapatite nano compound double drug loading porous scaffold
6	IN201305009-I4 (September 04, 2015), Parimanathu KRV et al.	Method for preparing nanoporous bioceramic portion for bone implantation
7	CN104587488-A (May 06, 2015), Cheng W et al.	Silica nanoparticles-pH-responsive liver cancer cells controlled drug delivery system
8	WO2014174437-A1 (October 30, 2014), Lilja M, Soerensen JH, et al.	Method for loading hydroxyapatite coated implants fixation pins, with antibiotics
9	CN103935973-A (April 29, 2014), Zhang Q et al.	Preparation of radial multi-structured nano-hydroxyapatite for use in biomedical field
10	WO2014141287-A1 (September 18,2014), Koyakutty M et al.	Doped nanobiomaterial as contrast agent for multi-functional medical imaging
11	WO2014124496-A1 (August 21, 2014), Dehghani F et al.	Composite material useful as bone and dental filler and injectable formulation
12	CN103041447-A (April 17, 2013), Pan H, Wang J	Injectable silk fibroin bone repair filling sustained-release material
13	US2012010599-A1 (January 12, 2012), Jin S, Smith G, Choi C	Inducing, enhancing, prolonging bone-forming capacity and drug delivery
14	CN102614529-A (August 01, 2012), Chen Y et al.	Drug delivery system for treating nasopharyngeal carcinoma
15	WO2012010520-A1 (January 26, 2012), Mueller WEG, Wiens M	Nano/microparticle used as a supplement for reducing tooth hypersensitivity
16	WO2009132411-A1 (November 05, 2009), TroczynskI T et al.	Polymer-free bioactive agent delivery system for implantable medical device
17	US2007190102-A1 (August 16, 2007), Luo P	Biocompatible implant for delivering drugs or proteins
18	US2005226939-A1 (October 13, 2005), Ramalingam M et al.	Method for production of nano-sized hydroxyapatite particles
19	US2003219466-A1 (November 27, 2003), Kumta PN et al.	Preparation of hydroxyapatite
20	US6165486-A (December 26, 2000), Marra KG et al.	Biocompatible osteoconductive composites supporting bone cell growth

all these aspects, nHAp can be considered as one of the most promising, efficient drug delivery bioceramics of present time.

The potentials of nHAp and related CaP ceramics in drug delivery applications are not only highlighted in a vast number of recent publications but also demonstrated through filed and offered patents during 2000–2017. The registered patents granted during this period are enlisted in Table 5:

Prospects of HAp Nanostructures

Nanophase HAp bioceramics have extended their prominence in biomedical field due to their superior biological and biomechanical properties. Development of biocompatible nHAp with desired characteristics would be greatly benefited from the recent advances in nanotechnology. Although several methods have been evolved for synthesizing HAp at nanoscale in the past two decades, current techniques face a number of limitations, such as serious aggregation and agglomeration of particles, wide particle size dispersion, and their low specific surface area. To address these issues, new, improved synthesis routes have to be established. A significant amount of research in this area is expected to focus on the application of nHAp as resorbable scaffolds, which can replace endogenous hard tissues over time. In the future, the ability to functionalize nHAp surfaces with organic molecules of different natures and dimensions (chain lengths), as well as the ability to control the physical, chemical, and topographical properties of their surfaces will define their usefulness for selective targeting within biological systems, especially the specificity towards individual proteins and peptides. On the other hand, a better understanding of the influence of size, morphology, and nHAp—biological cell interfaces are essential for their direct applications in biotechnology. Effective collaboration of scientists of different disciplines is necessary to develop such a complicated interdisciplinary research. For the application as drug carriers, the nHAp must be able to store and retain a large amount of drug within their pores and release them in controlled manner. In that sense, the mesoporous HAp nanoparticles have a good prospect for drug delivery applications, provided their pore-architecture could be controlled for a sustained drug release.

Recent developments on plasmonic nanostructures, especially the plasmonic nanocomposites of core-shell nature, for example, magnetic-core@plasmonic-shell, ceramic-core@plasmonic-shell, and magnetic-core@plasmonic-shell@porous ceramic-shell shed a great hope for fabricating more complex nanostructures based on HAp and externally controlled (using infra-red, radio frequency, and other type of radiations) drug release at specific body sites.

CONCLUSIONS

The main objective of this review is to present state of the art on drug delivery applications of HAp nanostructures. It is already well established that HAp is an excellent biomaterial for various biomedical applications. However, utilization of HAp for specific drug delivery application requires specific functionalities, which are difficult to introduce in its bulk form. Recent advances in nanofabrication technology opened up this possibility as HAp nanostructures of diverse morphology, size and compositions could be fabricated through different synthesis routes. Although there exists no consensus on which morphology of HAp nanostructures is most suitable for which kind of drug, researchers have investigated the drug delivery capabilities of HAp nanostructures of different morphologies, utilizing different types of drugs, including antibiotics, anticancer, analgesic, anti-inflammatory, etc. Mesoporous HAp nanostructures are seen to have excellent prospects in drug delivery applications due to their high surface area and high pore volume. On the other hand, added functionalities could be introduced to HAp nanostructures through doping them by rare-earth ions, alloying them with magnetic materials such as magnetite, or designing new geometries such as core-shell structures of HAp and non-CaP materials. While all these modifications provide added functionalities to HAp or HAp-based nanostructures to make them multifunctional, further improvements, both in design and synthesis techniques, are necessary for fabricating the optimum structures with controlled unrelenting drug release properties. However, modified nHAps, such as rare-earth doped and magnetic functionally induced ones revealed a clear advantage for their utility for tissue imaging through fluorescence enhancement and MRI contrast, respectively. In this review, we tried to highlight most of the path-breaking recent works reported in the literature, highlighting their findings and conclusions, along with the history of the development and clinical use of bioceramics. However, the prospects of novel biomaterials such as HAp in biomedical fields definitely depend upon the advancement of our knowledge, not only of the material, but also its interactions with specific bio-molecules, cells, and tissues.

ACKNOWLEDGMENTS

REFERENCES

1. Dorozhkin SV. A detailed history of calcium ortho-phosphates from 1770s till 1950. *Mater Sci Eng C* 2013, 33:3085–3110.

2. Huebsch N, Mooney DJ. Inspiration and application in the evolution of biomaterials. *Nature* 2009, 462:426–432.

3. Ring ME. *Dentistry: An Illustrated History*. New York: Harry N Abrams; 1992, 320.

4. Bobbio A. The first endosseous alloplastic implant in the history of man. *Bull Hist Dent* 1970, 20:1–6.

5. Dressmann H. Ueber knochenplombierung bei hohlenformigen defekten des knochens. *Beitr Klin Chir* 1892, 9:804–810.

6. Anderson JMJ. The future of biomedical materials. *Mater Sci Mater Med* 2006, 17:1025–1028.

7. Albee FH. Studies in bone growth triple calcium phosphate as a stimulus to osteogenesis. *Ann Surg* 1920, 71:32–39.

8. Nery EB, Lynch KL, Hirthe WM, Mueller KH. Bioceramic implants in surgically produced infrabony defects. *J Periodontol* 1975, 46:328–347.

9. Fernândez E, Gil FJ, Ginebra MP, Driessens FCM, Planell JA. Best SM. Calcium phosphate bone cements for clinical applications, part II: precipitate formation during setting reactions. *J Mater Sci Mater Med* 1999, 10:177–183.

10. Shojai MS, Khorasani MT, Khoshdargi ED, Jamshidi A. Synthesis methods for nanosized hydroxyapatite with diverse structures. *Acta Biomater* 2013, 9:7591–7621.

11. Dorozhkin SV. Calcium orthophosphates. *J Mater Sci* 2007, 42:1061–1095.

12. Dorozhkin SV. Calcium orthophosphates in nature, biology and medicine. *Materials* 2009, 2:399–498.

13. Cellet TSP, Pereira GM, Muniz EC, Silva R, Rubira AF. Hydroxyapatite nano whiskers embedded in chondroitin sulfate microspheres as colon targeted drug delivery systems. *J Mater Chem B* 2015, 3:6837–6846.

14. Tiwari G, Tiwari R, Sriwastawa B, Bhati L, Pandey S, Pandey P, Bannerjee SK. Drug delivery systems: an updated review. *Int J Pharma Investig* 2012, 2:2–11.

15. Mattie DR, Bajpai PK. Analysis of the biocompatibility of ALCAP ceramics in rat femurs. *J Biomed Mater Res* 1988, 22:1101–1126.

16. Benghuzzi HA, England BG, Bajpai PK. Controlled release of hydrophillic compounds by resorbable and biodegradable ceramic drug delivery devices. *Biomed Sci Instrum* 1992, 28:179–182.

17. Pories WJ, Henzel JH, Rob CG, Strain WH. Acceleration of wound healing with zinc sulfate. *Ann Surg* 1967, 165:432–436.

18. Lambotte JC, Thomazeau H, Cathelineau G, Lancien G, Minet J, Langlais F. Tricalcium phosphate, an antibiotic carrier: a study focused on experimental osteomyelitis in rabbits. *Chirurgie* 1998, 123:572–579.

19. Guicheux J, Gauthier O, Aguado E, Pilet P, Couillaud S, Jegou D, Daculsi G, Heymann D. Human growth hormone locally released in bone sites by calcium phosphate biomaterial stimulates ceramic bone substitution without systemic effects: a rabbit study. *J Bone Miner Res* 1998, 13:739–748.

20. Nunnery M, Benghuzzi H, Tucci M, Zizzi T, Cason Z, England B, Hughes J. Histopathological evaluation of female reproductive tract exposed to sustained delivery of DHEA, and DHEA + E. *Biomed Sci Instrum* 1999, 35:79–84.

21. Zizzi T, Nunnery M, Cason Z, Tucci M, Benghuzzi H. The effects of dehydroepiandrosterone and dehydroepiandrosterone sulfate on the reproductive and vital organs of male rats. *Biomed Sci Instrum* 1999, 35:279–284.

22. Cason Z, Tucci M, England B, Benghuzzi H. TCPL delivery devices: endometrial changes associated with exogenous sustained release of ovarian hormones. *Biomed Sci Instrum* 1999, 35:205–210.

23. Otsuka M, Matsuda Y, Kokubo T, Yoshihara S, Nakamura T, Yamamuro T. Drug release from a novel self-setting bioactive glass cement containing cephalexin and its physicochemical properties. *J Biomed Mater Res* 1995, 29:33–38.

24. Albanese A, Tang PS, Chan WCW. The effect of nanoparticle size, shape, and surface chemistry on biological systems. *Annu Rev Biomed Eng* 2012, 14:1–16.

25. Nevozhay D, Kañska U, Budzyñska R, Boratyñski J. Current status of research on conjugates and related drug delivery systems in the treatment of cancer and other diseases (Polish). *Postepy Hig Med Dosw* 2007, 61:350–360.

26. Huang X, Li L, Liu T, Hao N, Liu H, Chen D, Tang F. The shape effect of mesoporous silica nanoparticles on bio distribution, clearance, and biocompatibility in vivo. *ACS Nano* 2011, 5:5390–5399.

27. Fadeel B, Bennett AEG. Better safe than sorry: understanding the toxicological properties of inorganic nanoparticles manufactured for biomedical applications. *Adv Drug Deliv Rev* 2010, 62:362–374.

28. Decuzzi P, Gentile F, Granaldi A, Curcio A, Causa F, Indolfi C, Netti P, Ferrari M. Flow chamber analysis of size effects in the adhesion of spherical particles. *Int J Nanomedicine* 2007, 2:689–696.

29. Gentile F, Curcio A, Indolfi C, Ferrari M, Decuzzi P. The margination propensity of spherical particles for vascular targeting in the microcirculation. *J Nanobiotechnol* 2008, 6:9.

30. Gupta AS. Role of particle size, shape, and stiffness in design of intravascular drug delivery systems: insights from computations, experiments, and nature. *WIREs Nanomed Nanobiotechnol* 2016, 8:255–270.

31. Son SJ, Appleford M, Ong JL, Wenke JC, Kim JM, Choi SH. Porous hydroxyapatite scaffold with three-dimensional localized drug delivery system using biodegradable microspheres. *J Control Release* 2011, 153:133–140.

32. Harding IS, Rashid N, Hing KA. Surface charge and the effect of excess calcium ions on the hydroxyapatite surface. *Biomaterials* 2005, 26:6818–6826.

33. Harris JM, Chess RB. Effect of pegylation on pharmaceuticals. *Nat Rev Drug Discov* 2003, 2:214–221.

34. Wahajuddin AS. Superparamagnetic iron oxide nanoparticles: magnetic nanoplatforms as drug carriers. *Int J Nanomedicine* 2012, 7:3445–3471.

35. Sperling RA, Parak WJ. Surface modification, functionalization and bioconjugation of colloidal inorganic nanoparticles. *Phil Trans R Soc A* 2010, 368:1333–1383.

36. Miessler GL, Tarr DA. *Inorganic Chemistry*. Northfield, MN: Prentice Hall; 2004. ISBN: 0-13-035471-6.

37. Mobasherpour I, Heshajin MS, Kazemzadeh A, Zakeri M. Synthesis of nanocrystalline hydroxyapatite by using precipitation method. *J Alloys Compd* 2007, 430:330–333.

38. Zhang Y, Lu J. The transformation of single-crystal calcium phosphate ribbon like fibres to hydroxyapatite spheres assembled from nanorods. *Nanotechnology* 2008, 19:155608.

39. Tao J, Jiang W, Pan H, Xu X, Tang R. Preparation of large-sized hydroxyapatite single crystals using homogeneous releasing controls. *J Cryst Growth* 2007, 308:151–158.

40. Tas AC. Synthesis of biomimetic Ca-hydroxyapatite powders at 37°C in synthetic body fluids. *Biomaterials* 2000, 21:1429–1438.

41. Padmanabhan SK, Balakrishnan A, Chu MC, Lee YJ, Kim TN, Cho SJ. Sol–gel synthesis and characterization of hydroxyapatite nanorods. *Particuology* 2009, 7:466–470.

42. Ramanan SR, Venkatesh R. A study of hydroxyapatite fibers prepared via sol–gel route. *Mater Lett* 2004, 58:3320–3323.

43. Bose S, Saha SK. Synthesis of hydroxyapatite nanopowders via sucrose templated sol–gel method. *J Am Ceram Soc* 2004, 86:1055–1057.

44. Ruban Kumar A, Kalainathan S. Sol–gel synthesis of nanostructured hydroxyapatite powder in presence of polyethylene glycol. *Phys B Condens Matter* 2010, 405:2799–2802.

45. Bigi A, Boanini E, Rubini K. Hydroxyapatite gels and nanocrystals prepared through a sol–gel process. *J Solid State Chem* 2004, 177:3092–3098.

46. Jokić B, Mitrić M, Radmilović V, Drmanić S, Petrović R, Janaćković D. Synthesis and characterization of monetite and hydroxyapatite whiskers obtained by a hydrothermal method. *Ceram Int* 2011, 37:167–173.

47. Zhang H, Darvell BW. Synthesis and characterization of hydroxyapatite whiskers by hydrothermal homogeneous precipitation using acetamide. *Acta Biomater* 2010, 6:3216–3222.

48. Cihlar J, Castkova K. Direct synthesis of nanocrystalline hydroxyapatite by hydrothermal hydrolysis of alkylphosphates. In: Hofmann H, Rahman Z, Schubert U, eds. *Nanostructured Materials*. Vienna: Springer; 2002. Print ISBN: 978-3-7091-7398-5. Online ISBN: 978-3-7091-6740-3.

49. Zhu K, Yanagisawa K, Onda A, Kajiyoshi K, Qiu J. Morphology variation of cadmium hydroxyapatite synthesized by high temperature mixing method under hydrothermal conditions. *Mater Chem Phys* 2009, 113:239–243.

50. Zhou W, Wang M, Cheung W, Guo B, Jia D. Synthesis of carbonated hydroxyapatite nanospheres through nanoemulsion. *J Mater Sci Mater Med* 2008, 19:103–110.

51. Lim G, Wang J, Ng S, Gan L. Formation of nanocrystalline hydroxyapatite in nonionic surfactant emulsions. *Langmuir* 1999, 15:7472–7477.

52. Lim G, Wang J, Ng S, Gan L. Nanosized hydroxyapatite powders from micro emulsions and emulsions stabilized by a biodegradable surfactant. *J Mater Chem* 1999, 9:1635–1639.

53. Jarudilokkul S, Tanthapanichakoon W, Boonamnuayvittaya V. Synthesis of hydroxyapatite

nanoparticles using an emulsion liquid membrane system. *Colloids Surf A* 2007, 296:149–153.

54. Ethirajan A, Ziener U, Chuvilin A, Kaiser U, Cölfen H, Landfester K. Biomimetic hydroxyapatite crystallization in gelatin nanoparticles synthesized using a miniemulsion process. *Adv Funct Mater* 2008, 18:2221–2227.

55. Li H, Zhu MY, Li LH, Zhou CR. Processing of nano-crystalline hydroxyapatite particles via reverse microemulsions. *J Mater Sci* 2008, 43:384–389.

56. Mechay A, Feki HEL, Schoenstein F, Jouini N. Nanocrystalline hydroxyapatite ceramics prepared by hydrolysis in polyol medium. *Chem Phys Lett* 2012, 541:75–80.

57. Shih WJ, Wang MC, Hon MH. Morphology and crystallinity of the nanosized hydroxyapatite synthesized by hydrolysis using cetyltrimethylammonium bromide (CTAB) as a surfactant. *J Cryst Growth* 2005, 275:e2339–e2344.

58. Vukomanovic M, Bracko I, Poljansek I, Uskokovic D, Skapin SD, Suvorov D. The growth of silver nanoparticles and their combination with hydroxyapatite to form composites via a sonochemical approach. *Cryst Growth Des* 2011, 11:3802–3812.

59. Jevtic M, Mitric M, Skapin S, Jancar B, Ignjatovic N, Uskokovic D. Crystal structure of hydroxyapatite nanorods synthesized by sonochemical homogeneous precipitation. *Cryst Growth Des* 2008, 8:2217–2222.

60. Kim W, Saito F. Sonochemical synthesis of hydroxyapatite from H$_3$PO$_4$ solution with Ca(OH)$_2$. *Ultrason Sonochem* 2001, 8:85–88.

61. Han Y, Li S, Wang X, Bauer I, Yin M. Sonochemical preparation of hydroxyapatite nanoparticles stabilized by glycosaminoglycans. *Ultrason Sonochem* 2007, 14:286–290.

62. Wasim M, Malik RS, Tufail MU, Jutt AU, Ahmad R, Deen KM. Synthesis and characterization of hydroxyapatite powder from natural bovine bone. *J Biomim Biomater Tissue Eng* 2014, 19:35–42.

63. Sahni G, Gopinath P, Jeevanandam P. A novel thermal decomposition approach to synthesize hydroxyapatite–silver nanocomposites and their antibacterial action against GFP-expressing antibiotic resistant *E. coli*. *Colloids Surf B Biointerfaces* 2013, 103:441–447.

64. Barralet J, Knowles JC, Best S, Bonfield W. Thermal decomposition of synthesized hydroxyapatite. *J Mater Sci Mater Med* 2002, 13:529–533.

65. Ozawa HM, Suzuki S. Microstructural development of natural hydroxyapatite originated from fish-bone waste through heat treatment. *J Am Ceram Soc* 2002, 85:1315–1317.

66. Cho JS, Kang YC. Nano-sized hydroxyapatite powders prepared by flame spray pyrolysis. *J Alloys Compd* 2008, 464:282–287.

67. Aizawa M, Hanazawa T, Itatani K, Howell F, Kishioka A. Characterization of hydroxyapatite powders prepared by ultrasonic spray-pyrolysis technique. *J Mater Sci* 1999, 34:2865–2873.

68. Wakiya N, Yamasaki M, Adachi T, Inukai A, Sakamoto N, Fu D, Sakurai O, Shinozaki K, Suzuki H. Preparation of hydroxyapatite–ferrite composite particles by ultrasonic spray pyrolysis. *Mater Sci Eng B* 2010, 173:195–198.

69. Hwang KS, Jeon KO, Jeon YS, Kim BH. Hydroxyapatite forming ability of electrostatic spray pyrolysis derived calcium phosphate nano powder. *J Mater Sci Mater Med* 2007, 18:619–622.

70. Sasikumar S, Vijayaraghavan R. Effect of metal-ion-to-fuel ratio on the phase formation of bioceramic phosphates synthesized by self-propagating combustion. *Sci Technol Adv Mater* 2008, 9:035003–035007.

71. Aghayan M, Rodríguez M. Influence of fuels and combustion aids on solution combustion synthesis of bi-phasic calcium phosphates (BCP). *Mater Sci Eng C* 2012, 32:2464–2468.

72. Ghosh SK, Roy SK, Kundu B, Datta S, Basu D. Synthesis of nano-sized hydroxyapatite powders through solution combustion route under different reaction conditions. *Mater Sci Eng B* 2011, 176:14–21.

73. Pratihar SK, Garg M, Mehra S, Bhattacharyya S. Phase evolution and sintering kinetics of hydroxyapatite synthesized by solution combustion technique. *J Mater Sci Mater Med* 2006, 17:501–1507.

74. Tas AC. Combustion synthesis of calcium phosphate bioceramic powders. *J Eur Ceram Soc* 2000, 20:2389–2394.

75. Pramanik S, Agarwal AK, Rai K, Garg A. Development of high strength hydroxyapatite by solid-state-sintering process. *Ceram Int* 2007, 33:419–426.

76. Zhang HG, Zhu Q. Preparation of fluoride-substituted hydroxyapatite by a molten salt synthesis route. *J Mater Sci Mater Med* 2006, 17:691–695.

77. Teshima K, Lee SH, Sakurai M, Kameno Y, Yubuta K, Suzuki T, Shishido T, Endo M, Oishi S. Well-formed one-dimensional hydroxyapatite crystals grown by an environmentally friendly flux method. *Cryst Growth Des* 2009, 9:2937–2940.

78. Tas AC. Molten salt synthesis of calcium hydroxyapatite whiskers. *J Am Ceram Soc* 2001, 84:295–300.

79. Silva C, Graça MPF, Valente M, Sombra ASB. Crystallite size study of nanocrystalline hydroxyapatite and ceramic system with titanium oxide obtained by dry ball milling. *J Mater Sci* 2007, 42:3851–3855.

80. Fahami A, Ebrahimi-Kahrizsangi R, Nasiri-Tabrizi B. Mechanochemical synthesis of hydroxyapatite/titanium nanocomposite. *Solid State Sci* 2011, 13:135–141.

81. Nasiri-Tabrizi B, Honarmandi P, Ebrahimi-Kahrizsangi R. Synthesis of nanosize single-crystal hydroxyapatite via mechanochemical method. *Mater Lett* 2009, 63:543–546.

82. El Briak-Ben Abdeslam H, Ginebra M, Vert M, Boudeville P. Wet or dry mechanochemical synthesis of calcium phosphates? Influence of the water content on DCPD–CaO reaction kinetics. *Acta Biomater* 2008, 4:378–386.

83. Fathi M, Mohammadi Zahrani E. Mechanical alloying synthesis and bioactivity evaluation of nanocrystalline fluoridated hydroxyapatite. *J Cryst Growth* 2009, 311:1392–1403.

84. Yeong B, Junmin X, Wang J. Mechanochemical synthesis of hydroxyapatite from calcium oxide and brushite. *J Am Ceram Soc* 2004, 84:465–467.

85. Mondal S, Mondal B, Dey A, Mukhopadhyay SS. Studies on processing and characterization of hydroxyapatite biomaterials from different bio wastes. *J Miner Mater Characterization Eng* 2012, 11:55–67.

86. Mondal S, Pal U, Dey A. Natural origin hydroxyapatite scaffold as potential bone tissue engineering substitute. *Ceram Int* 2016, 42:18338–18346.

87. Charlena SIH, Putri DK. Synthesis of hydroxyapatite from rice fields snail shell (*Bellamya javanica*) through wet method and pore modification using chitosan. *Proc Chem* 2015, 17:27–35.

88. Sobczak A, Kida A, Kowalski Z, Wzorek Z. Evaluation of the biomedical properties of hydroxyapatite obtained from bone waste. *Pol J Chem Technol* 2009, 11:37–43.

89. Mondal S, Bardhan R, Mondal B, Dey A, Mukhopadhyay SS, Guha R, Roy K, Roy S. Synthesis, characterization and in vitro cytotoxicity assessment of hydroxyapatite from different bioresources for tissue engineering application. *Bull Mater Sci, Bull Mater Sci* 2012, 35:683–691.

90. Mondal S, Mahata S, Kundu S, Mondal B. Processing of natural resourced hydroxyapatite ceramics from fish scale. *Adv Appl Ceram* 2010, 109:234–239.

91. Mondal S, Mondal A, Mandal N, Mondal B, Mukhopadhyay SS, Dey A, Singh S. Physico-chemical characterization and biological response of Labeo Rohita-derived hydroxyapatite scaffold. *Bioprocess Biosyst Eng* 2014, 37:1233–1240.

92. Doostmohammadi A, Monshi A, Fathi M, Braissant O. A comparative physicochemical study of bioactive glass and bone-derived hydroxyapatite. *Ceram Int* 2011, 37:1601–1607.

93. Vecchio KS, Zhang X, Massie JB, Wang M, Kim CW. Conversion of bulk seashells to biocompatible hydroxyapatite for bone implants. *Acta Biomater* 2007, 3:910–918.

94. Wu SC, Tsou HK, ChuanHsu H, KuangHsu S, Liou SP, FuHo W. A hydrothermal synthesis of egg shell and fruit waste extract to produce nanosized hydroxyapatite. *Ceram Int* 2013, 39:8183–8188.

95. Narasaraju TSB, Phebe DE. Some physioco-chemical aspects of hydroxyapatite. *J Mater Sci* 1996, 31:1–21.

96. Naray-Szabo S. The structure of apatite (CaF) $Ca_4(PO_4)_3$. *Z Kristallogr* 1930, 75:387–398.

97. Hendricks SB, Jefferson SB, Mosley VMZ. The crystal structures of some natural and synthetic apatite-like substances. *Kristallogr Cryst Mater* 1932, 81:352–369.

98. Posner AS, Perloff A, Diorio AF. Refinement of hydroxyapatite structure. *Acta Crystallogr* 1958, 11:308–309.

99. Corno M, Rimola A, Bolis V, Ugliengo P. Hydroxyapatite as a key biomaterial: quantum mechanical simulation of its surface in interaction with biomolecules. *Phys Chem Chem Phys* 2010, 12:6309–6329.

100. Mostafa NY, Brown PW. Computer simulation of stoichiometric hydroxyapatite: structureand substitutions. *J Phys Chem Solid* 2007, 68:431–437.

101. Furukawa T, Matsusue Y, Yasunaga T, Nakagawa Y, Okada Y, Shikinami Y, Okuno M, Nakamura T. Histomorphometric study on high-strength hydroxyapatite/poly (L-lactide) composite rods for internal fixation of bone fractures. *J Biomed Mater Res* 2000, 50:410–419.

102. Trombelli L, Simonelli A, Pramstaller M, Wikesjo UME, Farina R. Single flap approach with and without guided tissue regeneration and a hydroxyapatite biomaterial in the management of intraosseous periodontal defects. *J Periodontol* 2010, 81:1256–1263.

103. Strietzel FP, Reichart PA, Graf HL. Lateral alveolar ridge augmentation using a synthetic nano-crystalline hydroxyapatite bone substitution material (Ostim): preliminary clinical and histological results. *Clin Oral Implants Res* 2007, 18:743–751.

104. Ye Q, Ohsaki K, Li K, Li DJ, Zhu CS, Ogawa T, Tenshin S, Takano-Yamamoto T. Histological reaction to hydroxyapatite in the middle ear of rats. *Auris Nasus Larynx* 2001, 28:131–136.

105. Lv Q, Nair L, Laurencin CT. Fabrication, characterization, and in vitro evaluation of poly (lactic acid glycolic acid)/nano-hydroxyapatite composite microsphere-based scaffolds for bone tissue engineering in rotating bioreactors. *J Biomed Mater Res A* 2009, 91:679–691.

106. Suchanek W, Yoshimura M. Processing and properties of hydroxyapatite based biomaterials for use as hard tissue replacement implants. *J Mater Res* 1998, 13:94–117.

107. Wopenka B, Pasteris JD. A mineralogical perspective on the apatite in bone. *Mater Sci Eng C* 2005, 25:131–143.

108. Hou CH, Hou SM, Hsueh YS, Lin J, HC W, Lin FH. The in vivo performance of biomagnetic hydroxyapatite nanoparticles in cancer hyperthermia therapy. *Biomaterials* 2009, 30:3956–3960.

109. Li J, Yin Y, Yao F, Zhang L, Yao K. Effect of nano and micro hydroxyapatite/chitosan-gelatin network film on human gastric cancer cells. *Mater Lett* 2008, 62:3220–3223.

110. Purdy KJ, Embley TM, Takaii S, Nedwell DB. Rapid extraction of DNA and rRNA from sediments by a novel hydroxyapatite spin-column method. *Appl Environ Microbiol* 1996, 62:3905–3907.

111. Mondal S, De RME, Pal U. Plasmon induced enhanced photocatalytic activity of gold loaded hydroxyapatite nanoparticles for methylene blue degradation under visible light. *RSC Adv* 2017, 7:8633–8645.

112. Zahouily M, Abrouki Y, Bahlaouan B, Rayadh A, Sebti S. Hydroxyapatite: new efficient catalyst for the Michael addition. *Cat Com* 2003, 4:521–524.

113. DeLoach LD, Payne SA, Chase LL, Smith LK, Kway WL, Krupke WF. Evaluation of absorption and emission properties of Yb^{3+} doped crystals for laser applications. *IEEE J Quantum Electron* 1993, 29:1179–1191.

114. Li L, Liu YK, Tao JH, Zhang M, Pan HH, XR X, Tang RK. Surface modification of hydroxyapatite nanocrystallite by a small amount of terbium provides a biocompatible fluorescent probe. *J Phys Chem C* 2008, 112:12219–12224.

115. Bouhaouss A, Bensaoud A, Laghzizil A, Ferhat M. Effect of chemical treatments on the ionic conductivity of carbonate apatite. *Int J Inorg Mater* 2001, 3:437–441.

116. Mahabole MP, Aiyer RC, Ramakrishna CV, Sreedhar B, Khairnar R. Synthesis, characterization and gas sensing property of hydroxyapatite ceramic. *Bull Mater Sci* 2005, 28:535–545.

117. Lin K, Pan J, Chen Y, Cheng R, Xu X. Study the adsorption of phenol from aqueous solution on hydroxyapatite nanopowders. *J Hazard Mater* 2009, 161:231–240.

118. Hashimoto Y, Taki T, Sato T. Sorption of dissolved lead from shooting range soils using hydroxyapatite amendments synthesized from industrial byproducts as affected by varying pH conditions. *J Environ Manage* 2009, 90:1782–1789.

119. Queiroz AC, Santos JD, Monteiro FJ. Porous HA scaffolds for drug releasing. *Bioceramics* 2005, 17:407–410.

120. Rauschmann MA, Wichelhaus TA, Stirnal V, Dingeldein E, Zichner L, Schnettler R, Alt V. Nanocrystalline hydroxyapatite and calcium sulphate as biodegradable composite carrier material for local delivery of antibiotics in bone infections. *Biomaterials* 2005, 26:2677–2684.

121. Otsuka M, Yoneoka K, Matsuda Y, Fox JL, Higuchi WI, Sugiyama Y. Oestradiol release from self-setting apatitic bone cement responsive to plasma-calcium level in ovariectomized rats and its physicochemical mechanism. *J Pharm Pharmacol* 1997, 49:1182–1188.

122. Ducheyne P, Qiu Q. Bioactive ceramics: the effect of surface reactivity on bone formation and bone cell function. *Biomaterials* 1999, 20:2287–2303.

123. Doss SK. Surface properties of hydroxyapatite: I. The effect of various inorganic ions on the electrophoretic behavior. *J Dent Res* 1976, 55:1067–1075.

124. Zafirau W, Parker D, Billotte W, Bajpai PK. Development of a ceramic device for the continuous local delivery of steroids. *Biomed Sci Instrum* 1996, 32:63–70.

125. Shenoy BD, Udupa N, Nagarajkumari A. Implantable drug delivery systems for centchroman. *Indian J Pharm Sci* 1997, 59:246–250.

126. Knepper-Nicolai B, Reinstorf A, Hofinger I, Flade K, Wenz R, Pompe W. Influence of osteocalcin and collagen on the mechanical and biological properties of Biocement D. *Biomol Eng* 2002, 19:227–231.

127. Walduck AK, Opdebeeck JP, Benson HE, Prankerd R. Biodegradable implants for the delivery of veterinary vaccines: design, manufacture and antibody responses in sheep. *J Control Release* 1998, 51:269–280.

128. Paul W, Sharma CP. Development of porous spherical hydroxyapatite granules: application towards protein delivery. *J Mater Sci Mater Med* 1999, 10:383–388.

129. Ginebra MP, Traykova T, Planell JA. Calcium phosphate cements as bone drug delivery systems: a review. *J Control Release* 2006, 113:102–110.

130. Yang L, Sheldon BW, Webster TJ. Nanophase ceramics for improved drug delivery: current opportunities and challenges. *Am Ceram Soc Bull* 2010, 89:24–30.

131. Chen L, Mccrate JM, Lee JC, Li H. The role of surface charge on the uptake and biocompatibility of hydroxyapatite nanoparticles with osteoblast cells. *Nanotechnology* 2011, 22:105708.

132. Ginebra MP, Traykova T, Planell JA. Calcium phosphate cements: competitive drug carriers for the musculoskeletal system. *Biomaterials* 2006, 27:2171–2177.

133. Thevenot P, Hu W, Tang L. Surface chemistry influence implant biocompatibility. *Curr Top Med Chem* 2008, 8:270–280.

134. Kong L, Mu Z, Yu Y, Zhang L, Hu J. Polyethylenei-mine-stabilized hydroxyapatite nanoparticles modified with hyaluronic acid for targeted drug delivery. *RSC Adv* 2016, 6:101790–101799.

135. Feest TG. Low molecular weight dextran: a continuing cause of acute renal failure. *Br Med J* 1976, 2:1300.

136. Dong G, Sun JS, Yao CH, Jiang GJ, Huang CW, Lin FH. A study on grafting and characterization of HMDI-modified calcium hydrogenphosphate. *Biomaterials* 2001, 22:3179–3189.

137. Dupraz AMP, Meer SAT, de Wijn JR, Goedemoed JH. Biocompatibility screening of silane-treated hydroxyapatite powders, for use as filler in resorbable composites. *J Mater Sci Mater Med* 1996, 7:731–738.

138. Balasundaram G, Sato M, Webster TJ. Using hydroxyapatite nanoparticles and decreased crystallinity to promote osteoblast adhesion similar to functionalizing with RGD. *Biomaterials* 2006, 27:2798–2805.

139. Bellis SL. Advantages of RGD peptides for directing cell association with biomaterials. *Biomaterials* 2011, 32:4205–4210.

140. Matsumoto T, Okazaki M, Inoue M, Hamada Y, Taira M, Takahashi J. Crystallinity and solubility characteristics of hydroxyapatite adsorbed amino acid. *Biomaterials* 2000, 23:2241–2247.

141. Sawyer AA, Weeks DM, Kelpke SS, McCracken MS, Bellis SL. The effect of the addition of a polyglutamate motif to RGD on peptide tethering to hydroxyapatite and the promotion of mesenchymal stem cell adhesion. *Biomaterials* 2005, 26:7046–7056.

142. Itoh D, Yoneda S, Kuroda S, Kondo H, Umezawa A, Ohya K, Ohyama T, Kasugai S. Enhancement of osteogenesis on hydroxyapatite surface coated with synthetic peptide in vitro. *J Biomed Mater Res* 2002, 62:292–298.

143. Abbasi Aval N, Pirayesh Islamian J, Hatamian M, Arabfirouzjaei M, Javadpour J, Rashidi MR. Doxorubicin loaded large-pore mesoporous hydroxyapatite coated superparamagnetic Fe3O4 nanoparticles for cancer treatment. *Int J Pharm* 2016, 509:159–167.

144. Meme L, Santarelli A, Marzo G, Emanuelli M, Nocini PF, Bertossi D, Putignano A, Dioguardi M, Lo Muzio L, Bambini F. Novel hydroxyapatite biomaterial covalently linked to raloxifene. *Int J Immunopathol Pharmacol* 2014, 27:437–444.

145. Tang W, Zhao J, Sha B, Liu H. Adsorption and drug release based on b-cyclodextrin-grafted hydroxyapatite composite. *J Appl Polym Sci* 2013, 127:2803–2808.

146. Ryabenkova Y, Jadav N, Conte M, Hippler MFA, McLaren NL, Coates PD, Twigg P, Paradkar A. Mechanism of hydrogen-bonded complex formation between ibuprofen and nanocrystalline hydroxyapatite. *Langmuir* 2017, 33:2965–2967.

147. Queiroz AC, Santos JD, Monteiro FJ, Gibson IR, Knowles JC. Adsorption and release studies of sodium ampicillin from hydroxyapatite and glass-reinforced hydroxyapatite composites. *Biomaterials* 2001, 22:1393–1400.

148. Kim HW, Knowles JC, Kim HE. Hydroxyapatite porous scaffold engineered with biological polymer hybrid coating for antibiotic Vancomycin release. *J Mater Sci Mater Med* 2005, 16:189–195.

149. Slosarczyk A, Szymura-Oleksiak J, Mycek B. The kinetics of pentoxifylline from drug loaded hydroxyapatite implants. *Biomaterials* 2000, 21:1215–1221.

150. Panyam J, Labhasetwar V. Biodegradable nanoparticles for drug and gene delivery to cells and tissues. *Adv Drug Deliv Rev* 2003, 55:329–347.

151. Murugan R, Panduranga Rao K. Controlled release of antibiotics from surface modified coralline hydroxyapatite. *Trends Biomater Artif Organs* 2002, 16:43–45.

152. Cheng X, Kuhn L. Chemotherapy drug delivery from calcium phosphate nanoparticles. *Int J Nanomedicine* 2007, 2:667–674.

153. Nandi SK, Mukherjee P, Roy S, Kundu B, Kumar De D, Basu D. Local antibiotic delivery systems for the treatment of osteomyelitis-a review. *Mater Sci Eng C* 2009, 29:2478–2485.

154. Kim HW, Knowles JC, Kim HE. Hydroxyapatite/poly (ε-caprolactone) composite coatings on hydroxyapatite porous bone scaffold for drug delivery. *Biomaterials* 2004, 25:1279–1287.

155. Yammamura K, Iwata H, Yotsuyanagi T. Synthesis of antibiotic-loaded hydroxyapatite beads and in vitro drug release testing. *J Biomed Mater Res* 1992, 26:1053–1064.

156. Shinto Y, Uchida A, Korkusuz F, Araki N, Ono K. Calcium hydroxyapatite ceramic used as a delivery system for antibiotics. *J Bone Joint Surg* 1992, 74–B:600–604.

157. Itokazu M, Ohno T, Tanemori T, Wada E, Kato N, Watanabe K. Antibiotic-loaded hydroxyapatite blocks in the treatment of experimental osteomyelitis in rats. *J Med Microbiol* 1997, 46:779–783.

158. Leu CT, Luegmayr E, Freedman LP, Rodan GA, Reszka AA. Relative binding affinities of bisphosphonates for human bone and relationship to antiresorptive efficacy. *Bone* 2006, 38:628–636.

159. Papapoulos SE. Bisphosphonate actions: physical chemistry revisited. *Bone* 2006, 38:613–616.

160. Grossmann G, Grossmann A, Ohms G, Breuer E, Chen R, Golomb G, Cohen H, Hagele G, Classen R. Solid-state NMR of bisphosphonates adsorbed on hydroxyapatite. *Magn Reson Chem* 2000, 38:11–16.

161. Kajiwara H, Yamaza T, Yoshinari M, Goto T, Iyama S, Atsuta I, Akido M, Tanaka T. The bisphosphonate pamidronate on the surface of titanium stimulates bone formation around tibial implants in rats. *Biomaterials* 2005, 26:581–587.

162. Ong HT, Loo JSC, Boey FYC, Russell SJ, Ma J, Peng KW. Exploiting the high affinity phosphonate-hydroxyapatite nanoparticle interaction for delivery of radiation and drugs. *J Nanopart Res* 2008, 10:141–150.

163. Hirabayashi H, Fujisaki J. Bone-specific drug delivery systems: approaches via chemical modification of bone-seeking agents. *Clin Pharmacokinet* 2003, 42:1319–1330.

164. Hao X, Zhang C, Chen S, Li Z, Yang X, Liu H, Jia G, Liu D, Ge K, Liang XJ, et al. Hybrid mesoporous silica-based drug carrier nanostructures with improved degradability by hydroxyapatite. *ACS Nano* 2015, 9:9614–9625.

165. Yu J, Chu X, Cai Y, Tong P, Yao J. Preparation and characterization of antimicrobial nano-hydroxyapatite composites. *Mater Sci Eng C* 2014, 37:54–59.

166. Lian X, Liu H, Wang X, Xu S, Cui F, Bai X. Antibacterial and biocompatible properties of vancomycin-loaded nano-hydroxyapatite/collagen/poly (lactic acid) bone substitute. *Prog Nat Sci Mater Int* 2013, 23:549–556.

167. Ye F, Guo H, Zhang H, He X. Polymeric micelle-templated synthesis of hydroxyapatite hollow nanoparticles for a drug delivery system. *Acta Biomater* 2010, 6:2212–2218.

168. Palazzo B, Iafisco M, Laforgia M, Margiotta N, Natile G, Bianchi CL, Walsh D, Mann S, Roveri N. Biomimetic hydroxyapatite- drug nanocrystals as potential bone substitutes with antitumor drug delivery properties. *Adv Funct Mater* 2007, 17:2180–2188.

169. Venkatasubbu GD, Ramasamy S, Avadhani GS, Ramakrishnan V, Kumar J. Surface modification and paclitaxel drug delivery of folic acid modified polyethylene glycol functionalized hydroxyapatite nanoparticles. *Powder Technol* 2013, 235:437–442.

170. Kundu B, Ghosh D, Sinha MK, Sen PS, Balla VK, Das N, Basu D. Doxorubicin-intercalated nano-hydroxyapatite drug-delivery system for liver cancer: an animal model. *Ceram Int* 2013, 39:3557–3566.

171. Ma MY, Zhu YJ, Li L, Cao SW. Nanostructured porous hollow ellipsoidal capsules of hydroxyapatite and calcium silicate: preparation and application in drug delivery. *J Mater Chem* 2008, 18:2722–2727.

172. Li D, He J, Cheng W, Wu Y, Hu Z, Tian H, Huang Y. Redox-responsive nanoreservoirs based on collagen end-capped mesoporous hydroxyapatite nanoparticles for targeted drug delivery. *J Mater Chem B* 2014, 2:6089–6096.

173. Li D, Huang X, Wu Y, Li J, Cheng W, He J, Tian H, Huang Y. Preparation of pH-responsive mesoporous hydroxyapatite nanoparticles for intracellular controlled release of an anticancer drug. *Biomater Sci* 2016, 4:272–280.

174. Tang QL, Zhu YJ, Wu J, Chen F, Cao SW. Calcium phosphate drug nanocarriers with ultrahigh and adjustable drug-loading capacity: one-step synthesis, in situ drug loading and prolonged drug release. *Nanomed Nanotechnol Biol Med* 2011, 7:428–434.

175. Curtin CM, Cunniffe GM, Lyons FG, Bessho K, Dickson GR, Duffy GP, Fj O'B. Innovative collagen nano-hydroxyapatite scaffolds offer a highly efficient non-viral gene delivery platform for stem cell-mediated bone formation. *Adv Mater* 2012, 24:749–754.

176. Liu TY, Chen SY, Liu DM, Liou SC. On the study of BSA-loaded calcium-deficient hydroxyapatite nanocarriers for controlled drug delivery. *J Control Release* 2005, 107:112–121.

177. Xu Z, Zhang YL, Song C, LL W, Gao HW. Interactions of hydroxyapatite with proteins and its toxicological effect to Zebrafish embryos development. *PLoS One* 2012, 7:e32818.

178. Talal A, Waheed N, Al-Masri M, McKay IJ, Tanner KE, Hughes FJ. Absorption and release of protein from hydroxyapatite-polylactic acid (HA-PLA) membranes. *J Dentistry* 2009, 37:820–826.

179. Webster TJ, Ergun C, Doremus RH, Siegel RW, Bizios R. Enhanced functions of osteoblasts on nano-phase ceramics. *Biomaterials* 2000, 21:1803–1810.

180. Liu J, Wu Q, Ding Y. Self-assembly and fluorescent modification of hydroxyapatite nanoribbon spherulites. *Eur J Inorg Chem* 2005, 2005:4145–4149.

181. Zhang C, Li C, Huang S, Hou Z, Cheng Z, Yang P, Peng JL. Self-activated luminescent and mesoporous strontium hydroxyapatite nanorods for drug delivery. *Biomaterials* 2010, 31:3374–3383.

182. Chen F, Huang P, Zhu YJ, Wu J, Zhang CL, Cui DX. The photoluminescence, drug delivery and imaging properties of multifunctional Eu^{3+}/Gd^{3+} dual-doped hydroxyapatite nanorods. *Biomaterials* 2011, 32:9031–9039.

183. Freeman MW, Arrott A, Watson JHL. Magnetism in medicine. *J Appl Phys* 1960, 31:S404–S405.

184. Syamchan SS, Sony G. Multifunctional hydroxyapatite nanoparticles for drug delivery and multimodal molecular imaging. *Microchim Acta* 2015, 182:1567–1589.

185. Tran N, Webster TJ. Increased osteoblast functions in the presence of hydroxyapatite-coated iron oxide nanoparticles. *Acta Biomater* 2011, 7:1298–1306.

186. Guo YP, Guo LH, Y-bo Y, Ning CQ, Guo YJ. Magnetic mesoporous carbonated hydroxyapatite microspheres with hierarchical nanostructure for drug

delivery systems. *Chem Commun* 2011, 47:12215–12217.

187. Gu L, He X, Wu Z. Mesoporous Fe_3O_4/hydroxyapatite composite for targeted drug delivery. *Mater Res Bull* 2014, 59:65–68.

188. Uchida A, Shinto Y, Araki N, Ono K. Slow release of anticancer drugs from porous calcium hydroxyapatite ceramic. *J Orthop Res* 1992, 10:440–445.

189. Mohammad NF, Othman R, Yeoh FY. Nanoporous hydroxyapatite preparation methods for drug delivery applications. *Rev Adv Mater Sci* 2014, 38:138–147.

190. Palazzo B, Sidoti MC, Roveri N, Tampieri A, Sandri M, Bertolazzi L, Galbusera F, Dubini G, Vena P, Contro R. Controlled drug delivery from porous hydroxyapatite grafts: an experimental and theoretical approach. *Mater Sci Eng C* 2005, 25:207–213.

191. Dai CF, Li SP, Li XD. Synthesis of nanostructured methotrexate/hydroxyapatite: morphology control, growth mechanism, and bioassay explore. *Colloids Surf B Biointerfaces* 2015, 136:262–271.

192. Itokazu M, Sugiyama T, Ohno T, Wada E, Katagiri Y. Development of porous apatite ceramic for local delivery of chemotherapeutic agents. *J Biomed Mater Res* 1998, 39:536–538.

193. Al-Sokanee ZN, Toabi AA, Al-Assadi MJ, Alassadi EA. The drug release study of ceftriaxone from porous hydroxyapatite scaffolds. *AAPS Pharm SciTech* 2009, 10:772–779.

194. Nandi SK, Kundu B, Ghosh SK, Mandal TK, Datta S, De DK, Basu D. Cefuroxime-impregnated calcium phosphates as an implantable delivery system in experimental osteomyelitis. *Ceram Int* 2009, 35:1367–1376.

195. Lafisco M, Sandri M, Panseri S, Delgado-Lopez JM, Gomez- Morales J, Tampieri A. Magnetic bioactive and biodegradable hollow Fe-doped hydroxyapatite coated poly (L-lactic) acid micro-nanospheres. *Chem Mater* 2013, 25:2610–2617.

196. Panseri S, Cunha C, Dalessandro T, Sandri M, Giavaresi G, Marcacci M, Hung CT, Tampieri A. Intrinsically superparamagnetic Fe-hydroxyapatite nanoparticles positively influences osteoblast-like cell behaviour. *J Nanobiotechnol* 2012, 10:32–41.

197. Kuda O, Pinchulk N, Iyanchenko L, Parkhomey O, Sych O, Leonowicz WR, Sowka E. Effect of Fe_3O_4, Fe and Cu doping on magnetic properties and behaviour in physiological solution of biological hydroxyapatite/glass composite. *J Mater Process Technol* 2009, 209:1960–1964.

198. Liu Z, Wang Q, Yao S, Yang L, Yu S, Feng X, Li F. Synthesis and characterization of Tb^{3+}/Gd^{3+} dual-doped multifunctional hydroxyapatite nanaoparticle. *Ceram Int* 2014, 40:2613–2617.

199. Liu M, Liu H, Sun S, Li X, Zhou Y, Hou Z, Lin J. Multifunctional hydroxyapatite/Na(Y/Gd) F4: Yb^{3+}, Er^{3+} composite fibres for drug delivery and dual model imaging. *Langmuir* 2014, 30:1176–1182.

200. Syamchand SS, Priya S, Sony G. Hydroxyapatite nanocrystals dually doped with fluorescent and paramagnetic labels for bimodal (luminomagnetic) cell imaging. *Michrochim Acta* 2015, 182:1213–1221.

201. Liu H, Chen F, Xi P, Chen B, Huang L, Cheng J, Shao C, Wang J, Bai D, Zeng Z. Biocompatible fluorescent hydroxyapatite: synthesis and live cell imaging applications. *J Phys Chem C* 2011, 115:18538–18544.

202. Yang P, Quan Z, Li C, Kang X, Lian H, Lin J. Bioactive, luminescent and mesoporous europium-doped hydroxyapatite as drug carrier. *Biomaterials* 2008, 29:4341–4347.

203. Yang C, Yang P, Wang W, Wang J, Zhang M, Lin J. Solvothermal synthesis and characterization of Ln (Eu^{3+}, Tb^{3+}) doped hydroxyapatite. *J Colloid Interface Sci* 2008, 328:203–210.

204. Liu H, Xi P, Xie G, Chen F, Li Z, Bai D, Zeng Z. Biocompatible hydroxyapatite nanoparticles as a redox luminescence switch. *J Biol Inorg Chem* 2011, 16:1135–1140.

205. de Araujo Batista TS, Macedo ZS, de Oliveira PASC, Valerio MEG. Production and characterization of pure and Cr^{3+} –doped hydroxyapatite for biomedical applications as fluorescent probes. *J Mater Sci* 2007, 42:2236–2243.